IMPULSE is funded by the European Union's Horizon 2020 programme under grant agreement No. 871161

ELISS2023

ELI Summer School | 29 Aug – 1 Sep 2023
Dolní Břežany, Czech Republic

Laser driven x-ray sources – Generation and Characterisation

Chris Armstrong

Central Laser Facility, STFC Rutherford Appleton Laboratory, UK

30/08/2023

Dolní Břežany, Czech Republic

Science and Technology Facilities Council

STFC Rutherford Appleton Laboratory

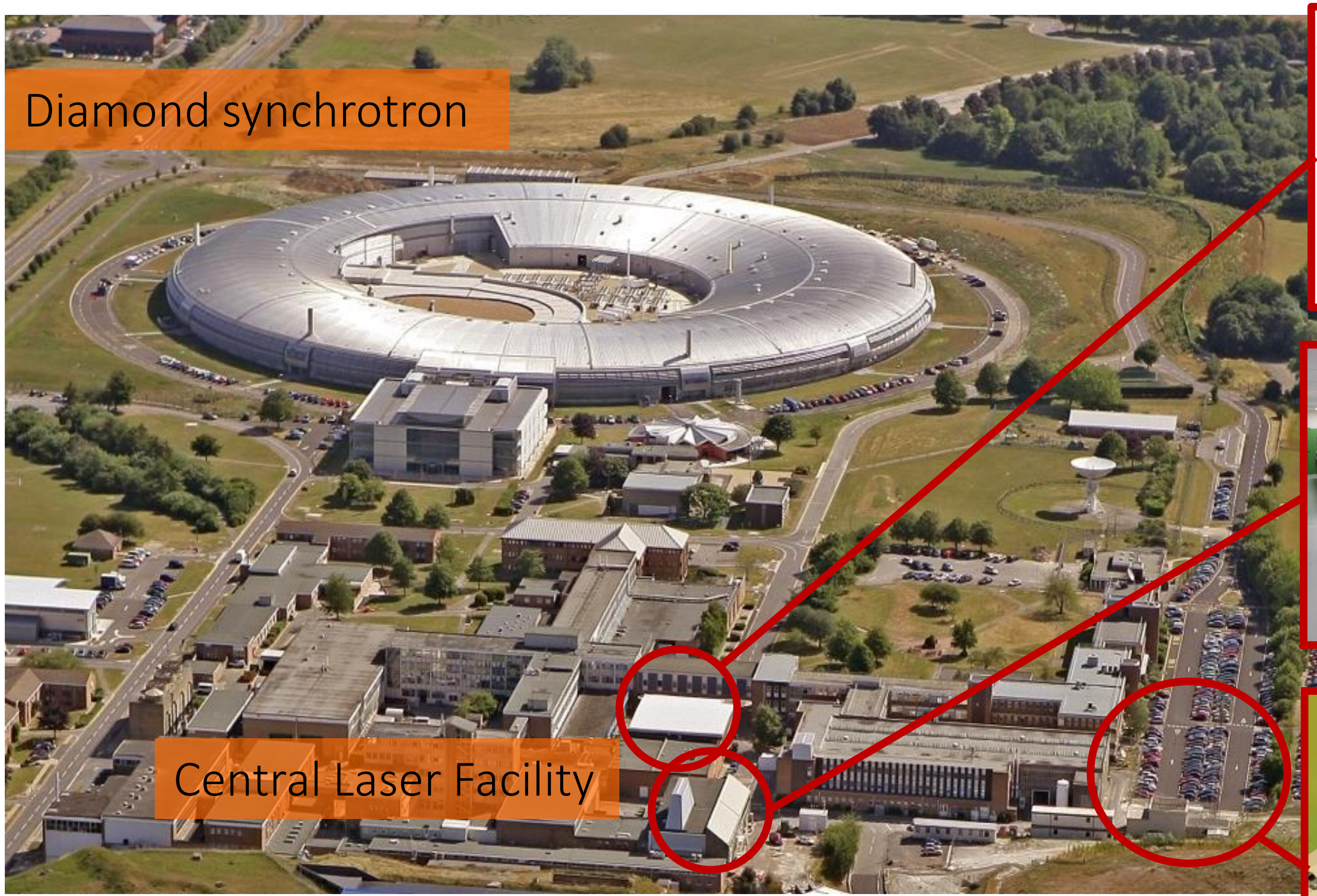

Vulcan

600J, 600fs, 1PW
10 shots a day

Gemini

2x15 J, 30 ps, 2x0.5PW
10 shots in 5 minutes

EPAC

30 J, 30 ps, 1PW
10 shots in 1 second
Due 2025

Science and Technology Facilities Council

central laser facility

Laser-plasma interactions

Solid Targets

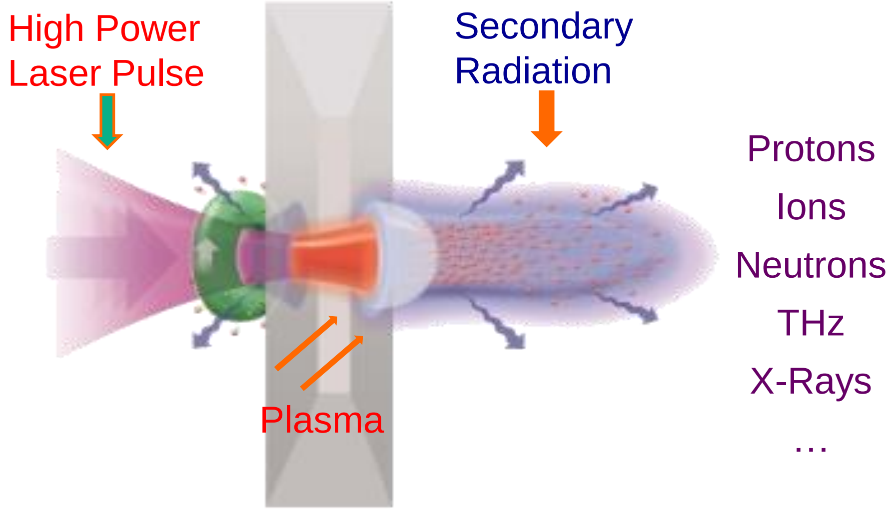

High efficiency (~80%), divergent, ~100um source of up to 100 MeV electrons, Ions, Neutrons, X-rays

Gas Targets

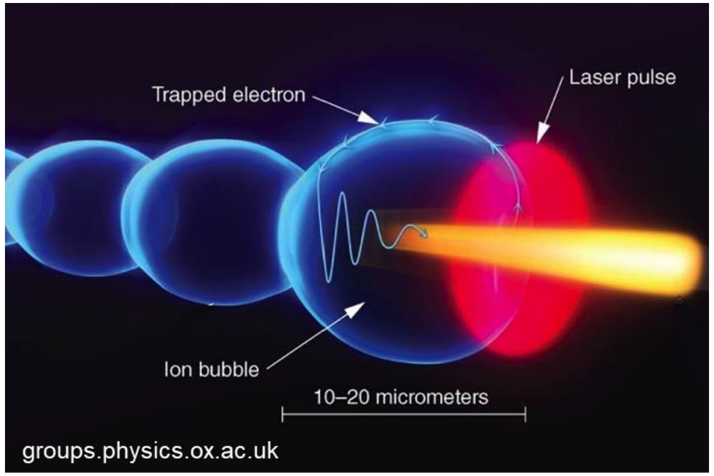

Low efficiency (~10%), highly directional, sub-micron source of up to 10 GeV electrons, and direct <100 keV coherent x-rays

Science and Technology Facilities Council

Laser driven x-ray sources

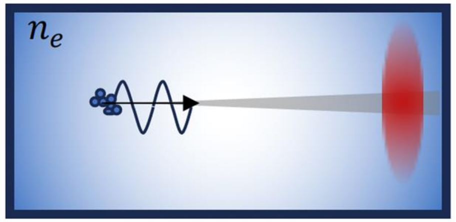

Betatron

10-100 keV
Narrowly divergence source
Due to electron orbits during acceleration

Inverse Compton Scattering

1-100s MeV
Narrowly divergence source
Due to scattering upshift of secondary laser

LWFA Bremsstrahlung

1-100s MeV
Semi divergent source
Interaction of ultra-relativistic electrons with target atoms

Science and Technology Facilities Council

central laser facility

Laser driven x-ray sources

Betatron

10-100 keV
Narrowly divergence source
Due to electron orbits during acceleration

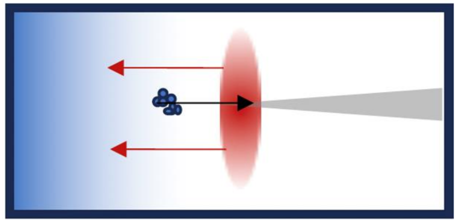

Inverse Compton Scattering

1-100s MeV
Narrowly divergence source
Due to scattering upshift of secondary laser

LWFA Bremsstrahlung

1-100s MeV
Semi divergent source
Interaction of ultra-relativistic electrons with target atoms

Science and Technology Facilities Council

central laser facility

Laser driven x-ray sources

Betatron

10-100 keV
Narrowly divergence source
Due to electron orbits during acceleration

Inverse Compton Scattering

1-100s MeV
Narrowly divergence source
Due to scattering upshift of secondary laser

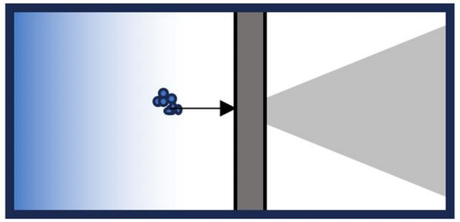

LWFA Bremsstrahlung

1-100s MeV
Semi divergent source
Interaction of ultra-relativistic electrons with target atoms

Science and Technology Facilities Council

Generation Mechanisms

Schemes to generate x-ray sources from LWFA

LWFA Betatron

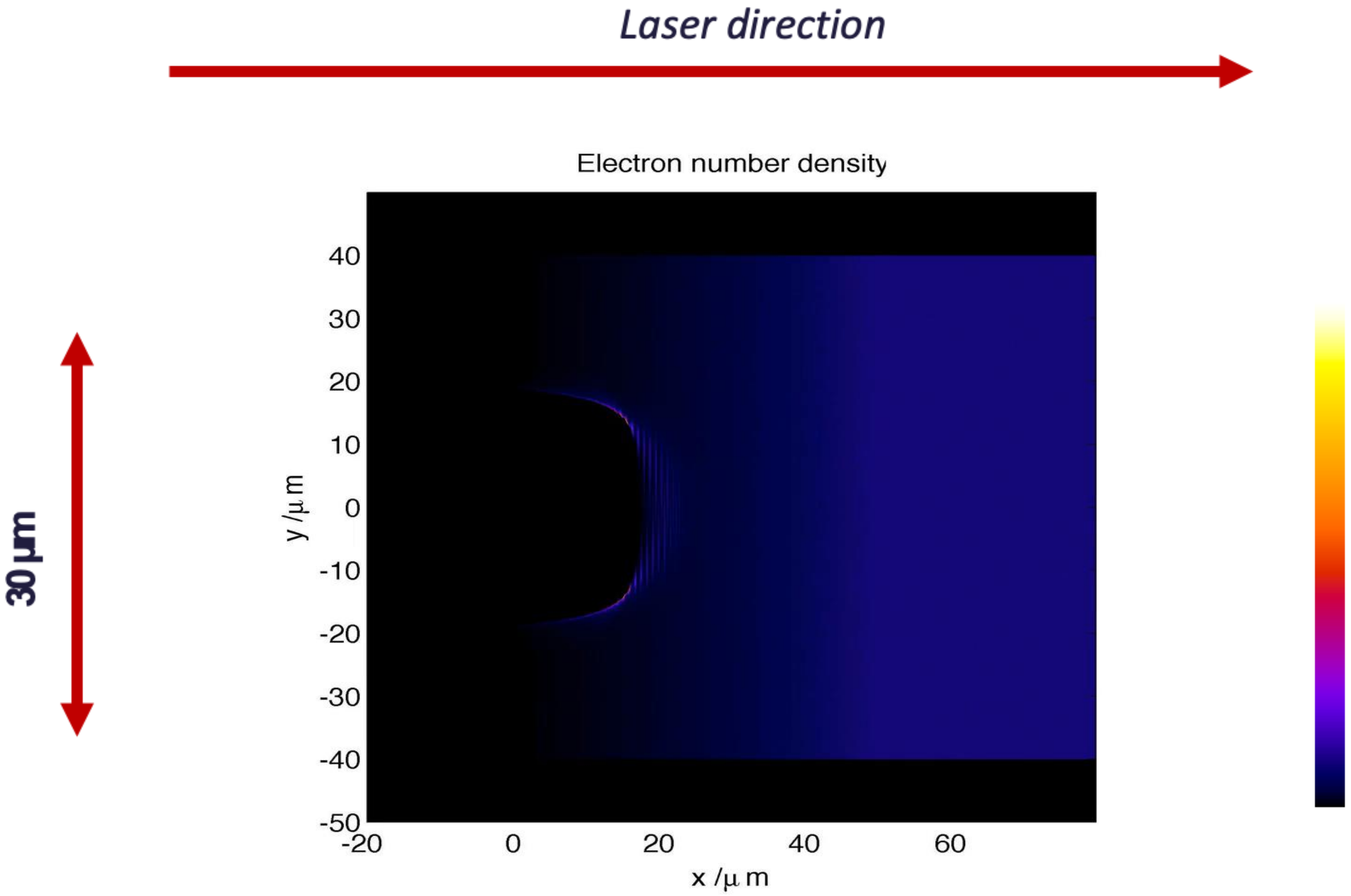

Electron density map from PIC simulation of LWFA

Laser wakefield acceleration

- cm-scale gas target
- Intense laser driver
- Multi-GeV electrons

Source of bright, pulsed radiation sources

- few fs duration
- µm-scale source size
- mrad divergence

LWFA Betatron

Electron energy ∝ Laser power,
plasma density
and wavelength

Critical Frequency ∝ Electron energy,
plasma frequency,
and orbit

Number of photons ∝ Electron number,
number of oscillators,
electron energy,
"Wiggle" factor

Spectral shape ∝ Angle,
electron energy,
Critical frequency

Critical energy

$$\omega_c \sim \frac{3}{2}\gamma^3 {k_\beta}^2 r_\beta c = \frac{3}{4c}\gamma^2 {\omega_p}^2 r_\beta$$

Total energy

$$W_{tot} = \frac{e^2}{6\epsilon_0} N_e N_\beta \gamma^2 K_\beta^2 k_\beta$$

Angular energy spectrum

$$\frac{d^2 I_B}{d\Omega d\theta_B} = \frac{\gamma^2\xi_B^2}{1+\gamma^2\theta_B^2}\left[K_{2/3}^2(\xi_B) + \frac{\gamma^2\xi^2}{1+\gamma^2\theta_B^2}K_{1/3}^2(\xi_B)\right]$$

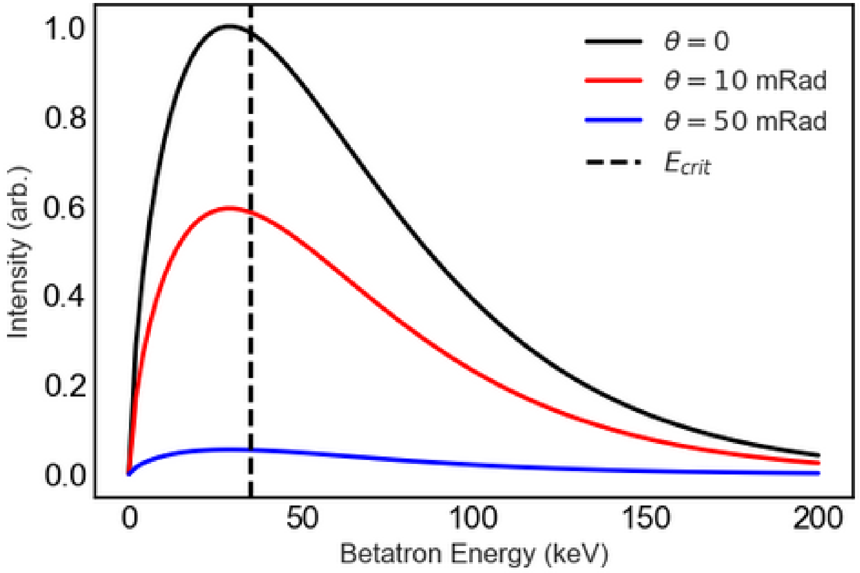

Science and Technology Facilities Council

~~Inverse~~ Compton Scattering (~~I~~CS)

For standard Compton scattering:

- Photon interactions with an electron at rest
- The photon is then scattered by some angle
- And experiences a downshift in energy relative to the angle of scatter.
- Electron recoils, conserving the momentum of the interaction

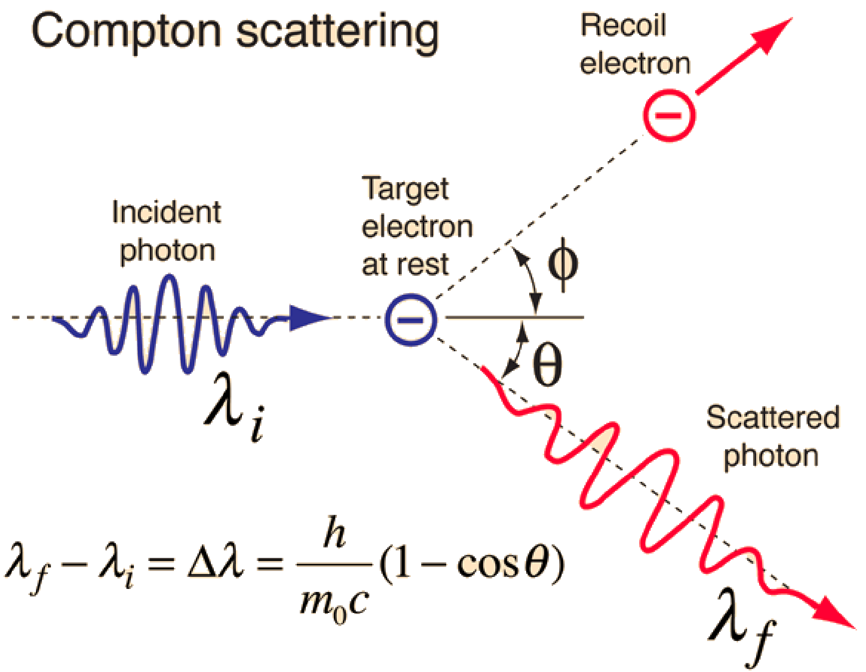

Inverse Compton Scattering (ICS)

For inverse Compton scattering, everything I just said but backwards:

- Photon interacts with a relativistic ($\gamma \gg 1$) electron
- Photon recoils from electron
- And experiences a upshift in energy relative to the angle of scatter and the energy of the electron

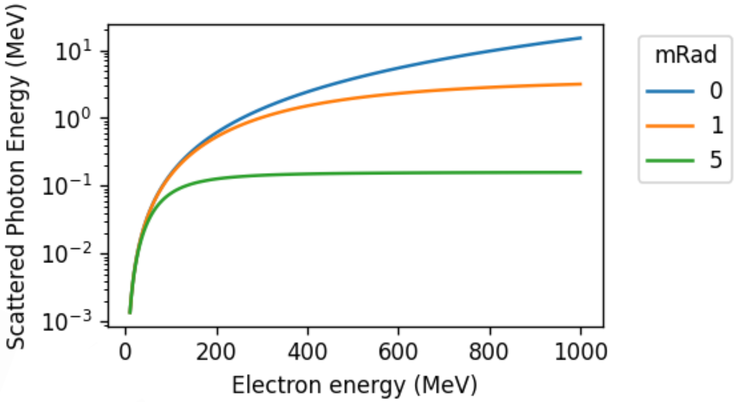

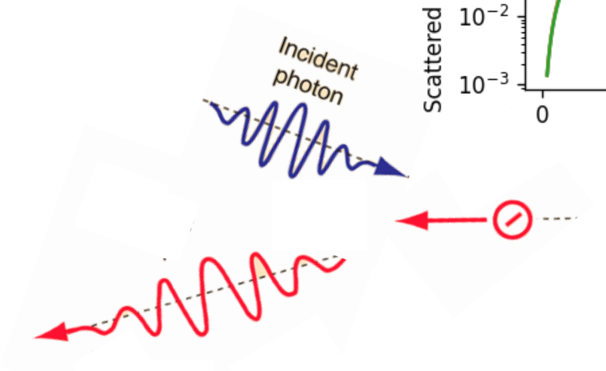

$$E_{x-ray} = \frac{4\gamma^2 E_{laser}}{1+(\gamma\theta)^2 + 4\gamma E_{laser}/(m_e c^2)}$$

On axis for large gamma this simplifies:

$$\approx 4\gamma^2 E_{laser} \qquad \gamma = \frac{E_e - m_0 c^2}{m_0 c^2}$$

Science and Technology Facilities Council

Inverse Compton Scattering (ICS)

The scaling is a combination of the driven electron conditions and the scattering laser:

Increases in the scattering laser/photon energy linearly maps to the scattered photon energy

Increases in the electron energy drive a *squared* scaling in scattered photon energy

Bandwidth of the emission maps from the bandwidth of the electron beam and the angle of incidence

Spectral width scales with electron bandwidth and interaction angle

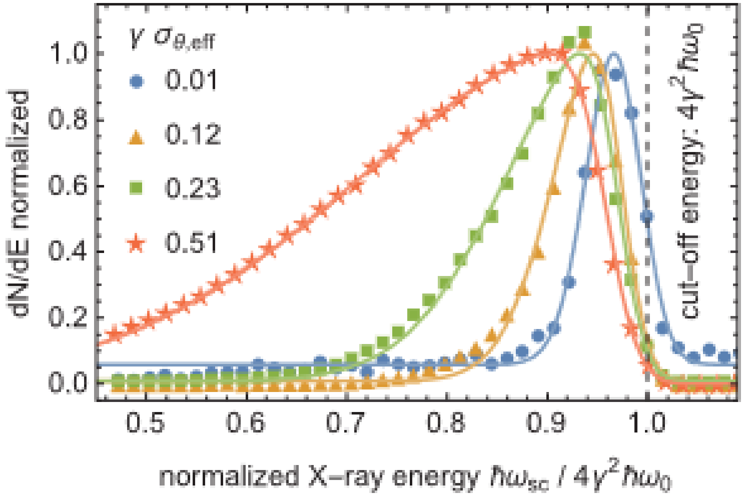

Kramer *et al.* Scientific Reports | (2018) 8:1398

Peak energy scales with electron energy

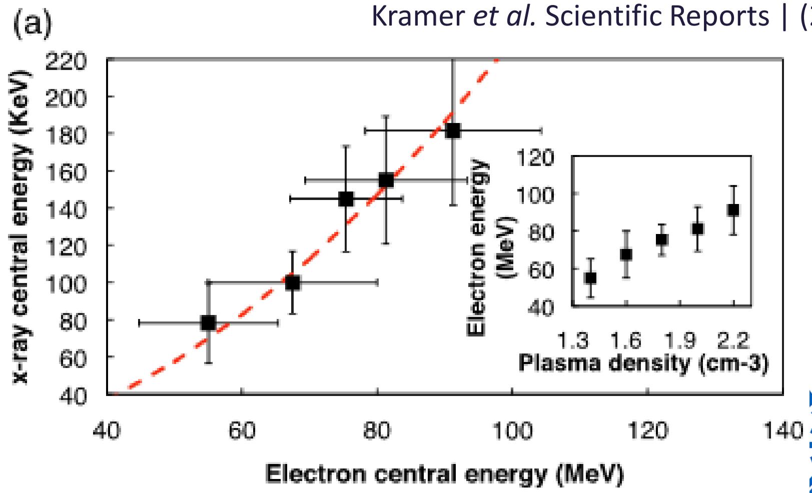

Tsai *et al.* Phys. Plasmas 22, 023106 (2015)

Science and Technology Facilities Council

LWFA Bremsstrahlung

Now instead of scattering a second laser onto the electron bunch we can accelerate them directly into a high-z target.

Electrons generate bremsstrahlung through interactions with the solid target, some remaining electron population escapes with a scattered fraction.

X-ray energy can't exceed the incident energy of the electrons, forms a distribution of x-ray energies of the form:

$$\frac{dN}{dE} \propto (E_x)^{-\frac{2}{3}} \exp\left(-\frac{E_x}{T_x}\right)$$

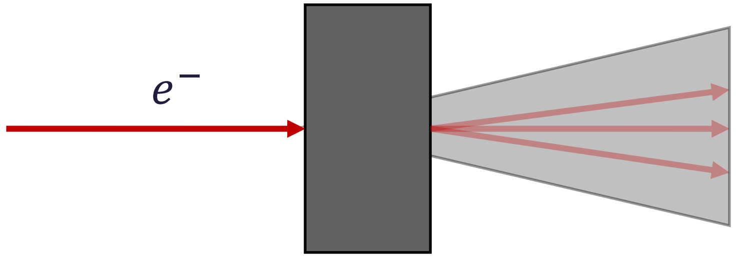

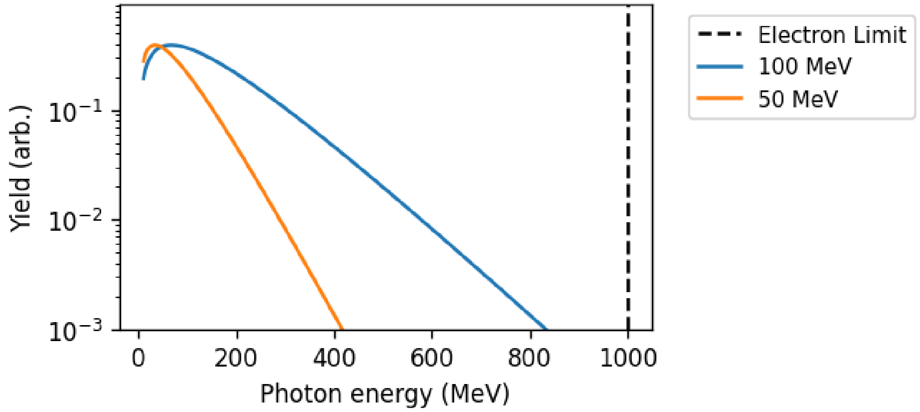

Science and Technology Facilities Council

central laser facility

Summary of Mechanisms

LWFA Betatron | ***Inverse Compton Scattering*** | ***LWFA Bremsstrahlung***

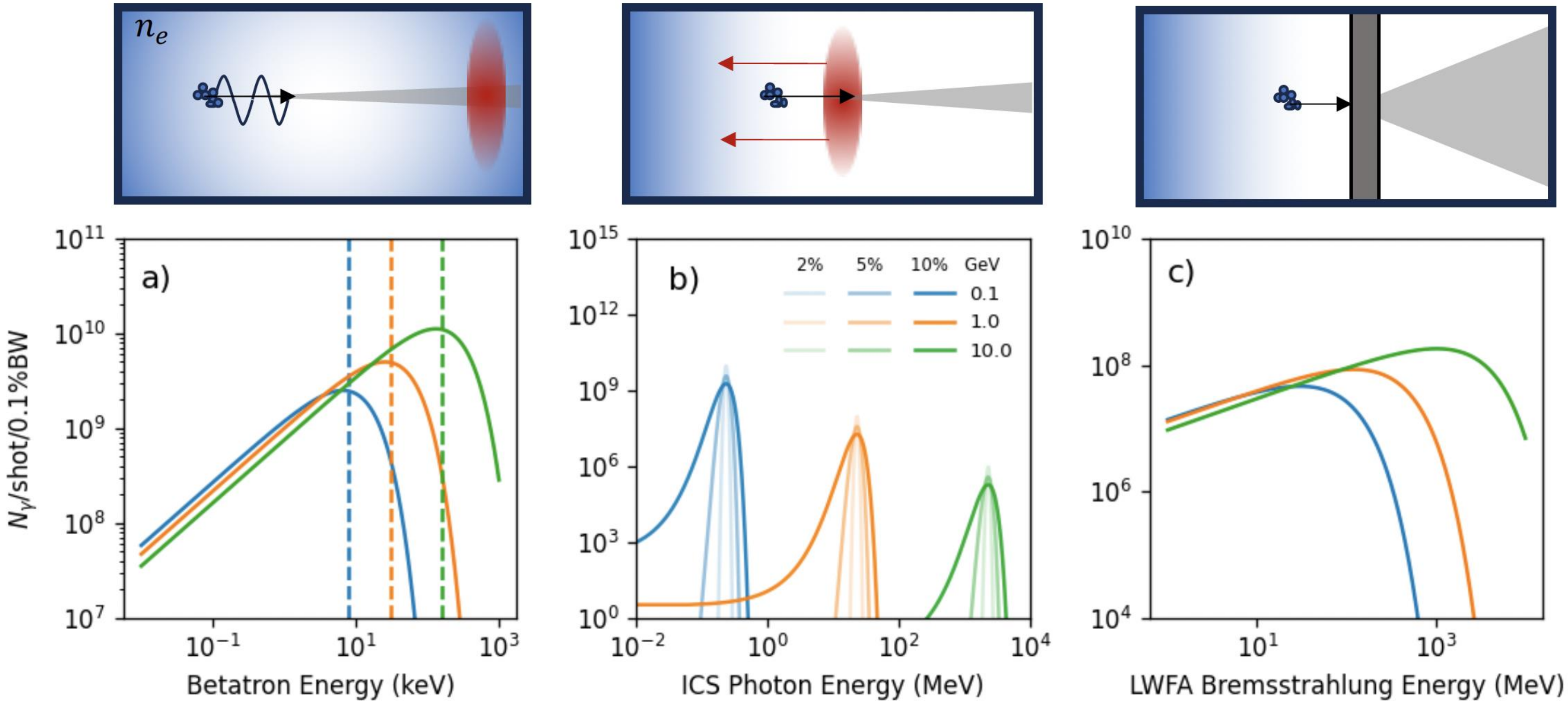

Science and Technology Facilities Council

Science and Technology Facilities Council

Characterisation

Methods to characterise emission from laser-driven sources

Science and Technology Facilities Council

Spectral Characterisation

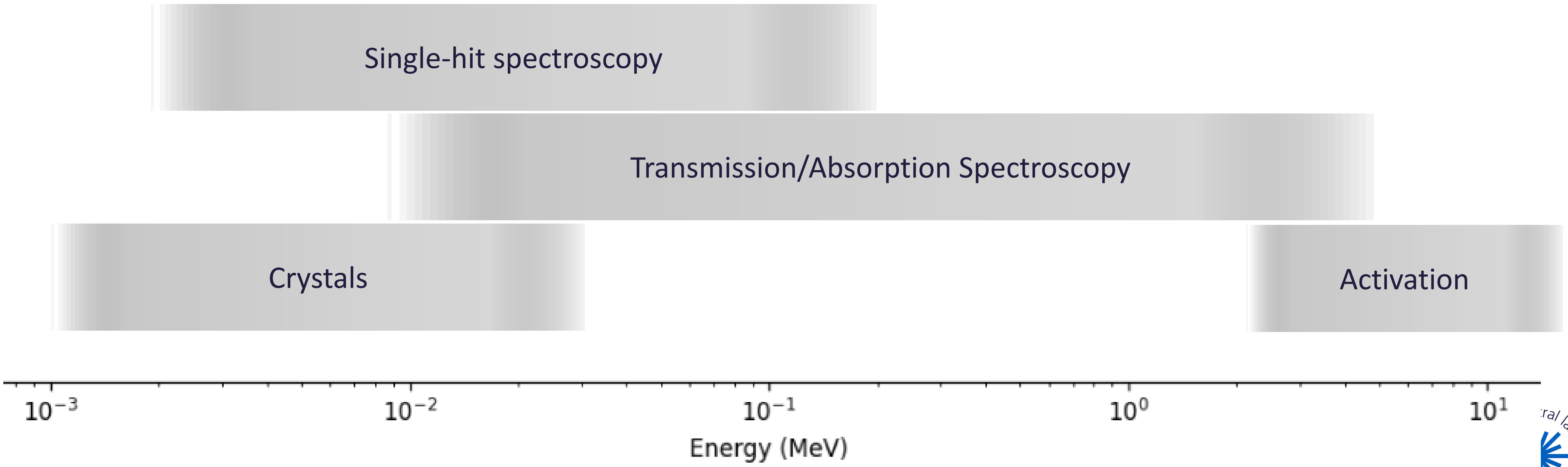

Spectral Characterisation

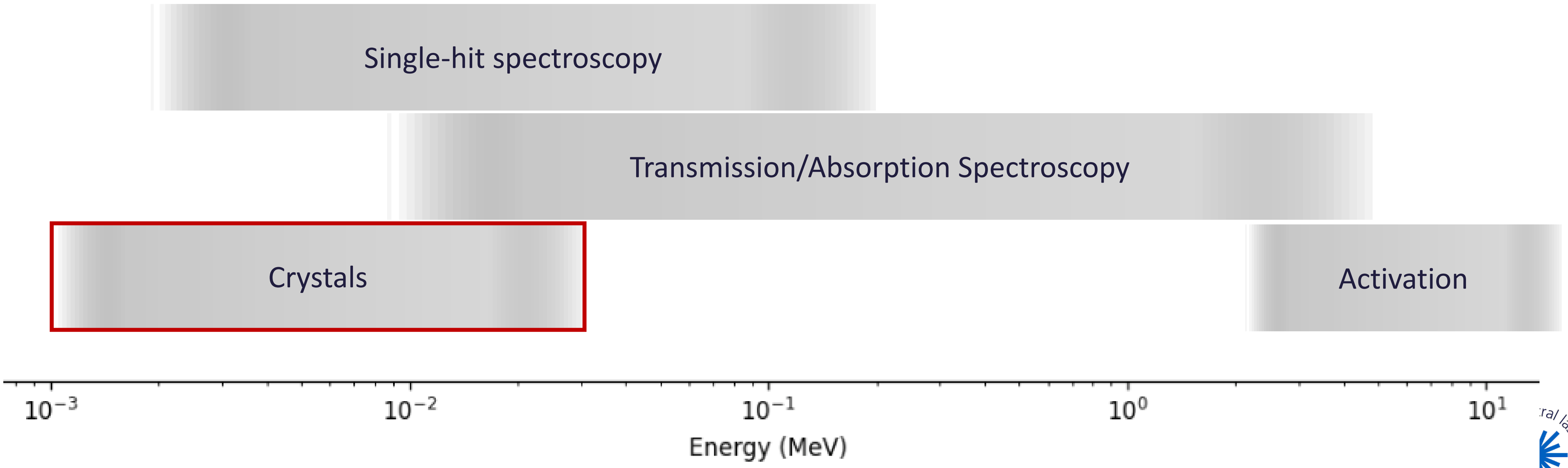

Crystal spectroscopy

X-rays interacting with an atomic lattice can lead to constructive interference at a specific angle

This angle defined by Braggs Law is dependent on the crystal spacing and the energy/wavelength of photon interacting with it.

This phenomena can be used to select energies of x-ray by angling the crystal to match the desired wavelength.

Curved crystals (in one or two planes) then permit selective imaging.

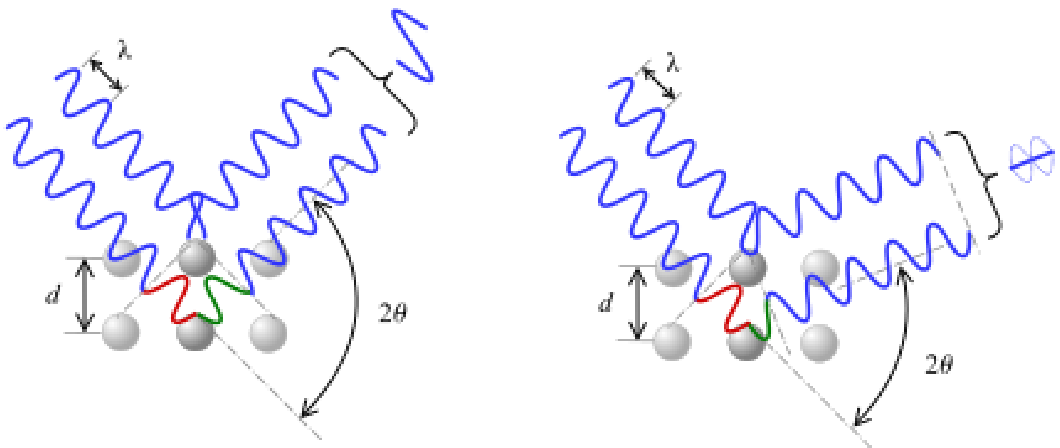

$$n\lambda = 2d\,\sin(\theta)$$

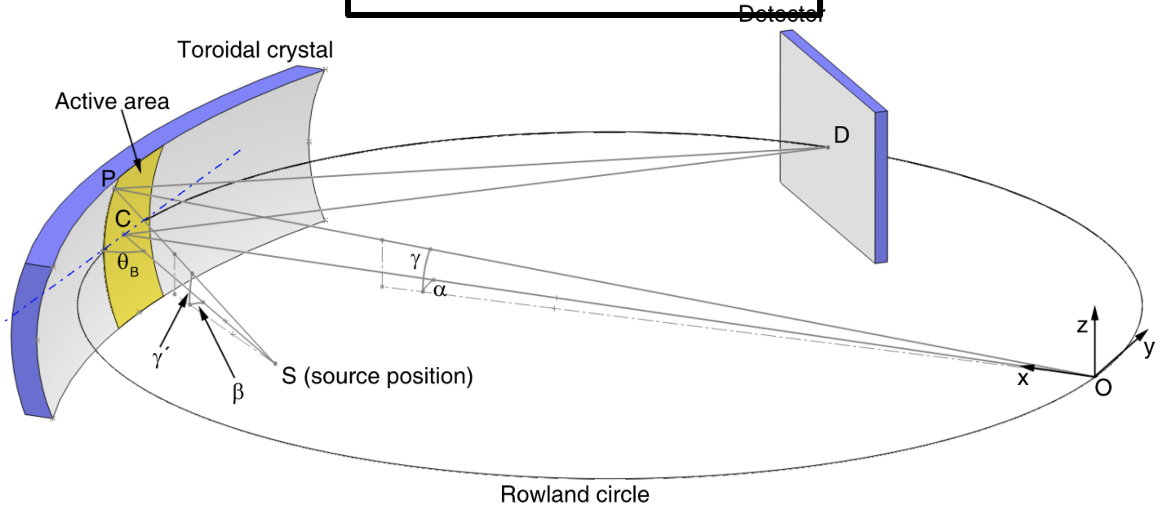

Imaging crystal will focus one energy (wavelength) to the detector

Science and Technology Facilities Council

Science and Technology Facilities Council

Spectral Characterisation

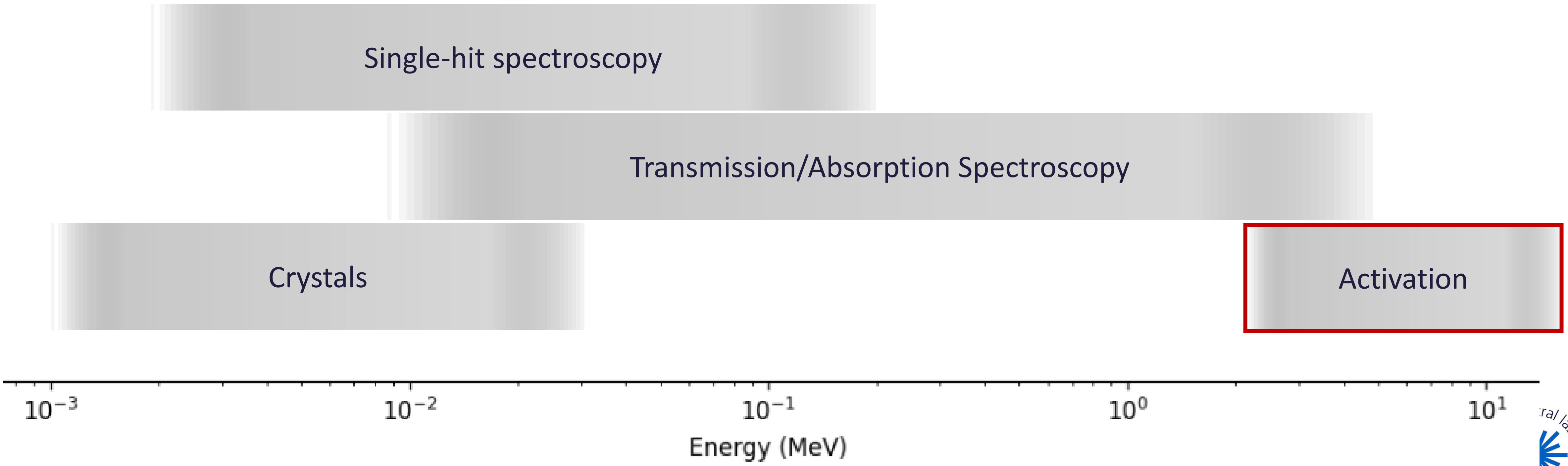

Activation spectroscopy

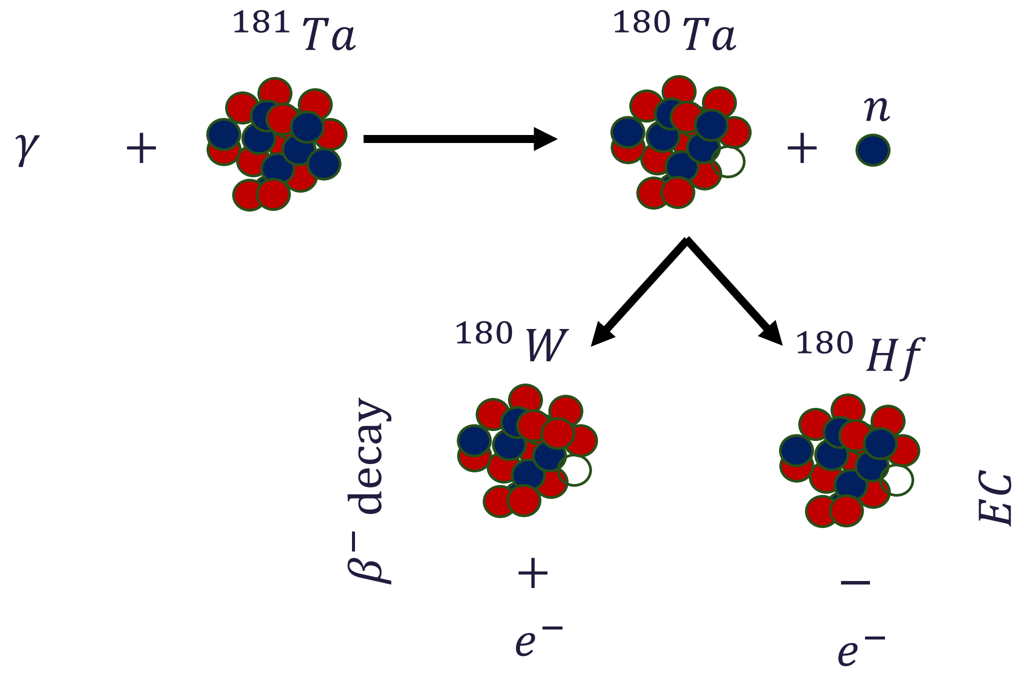

Nuclear activation occurs as a high energy photon (>10 MeV) interacts with a nucleus. There are several paths but the most common is (γ, n) reactions whereby the photon *kicks out* a neutron leaving the atom in a *generally unstable state.*

Monitoring the re-emission from the secondary products gives us a way to infer how many high energy photons there must have been

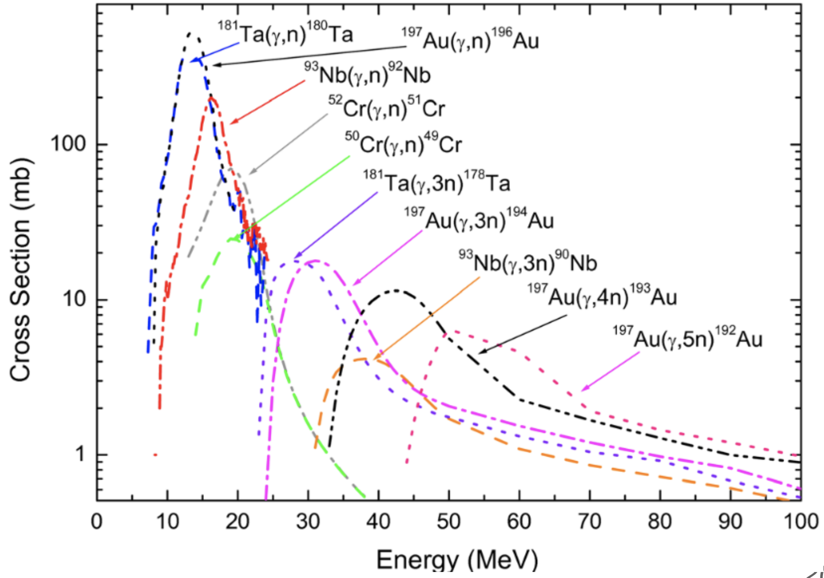

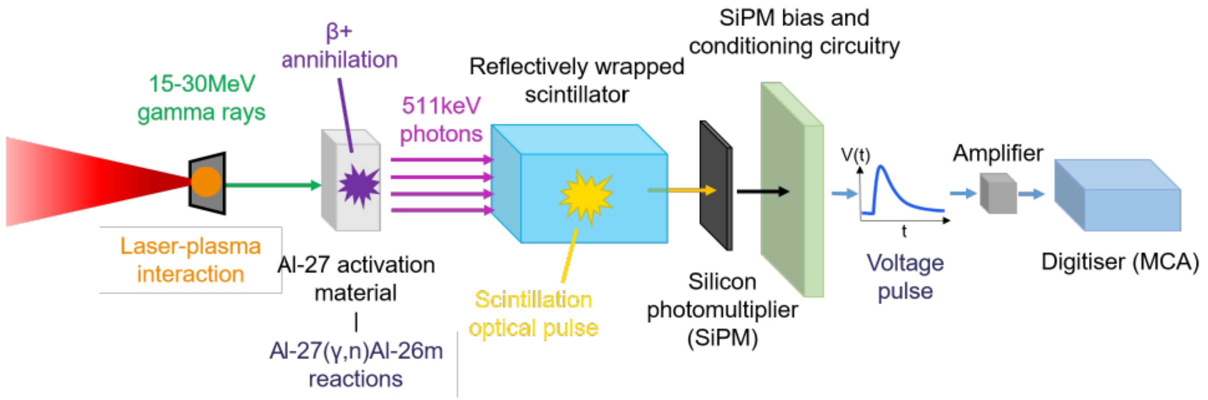

Spectral Characterisation

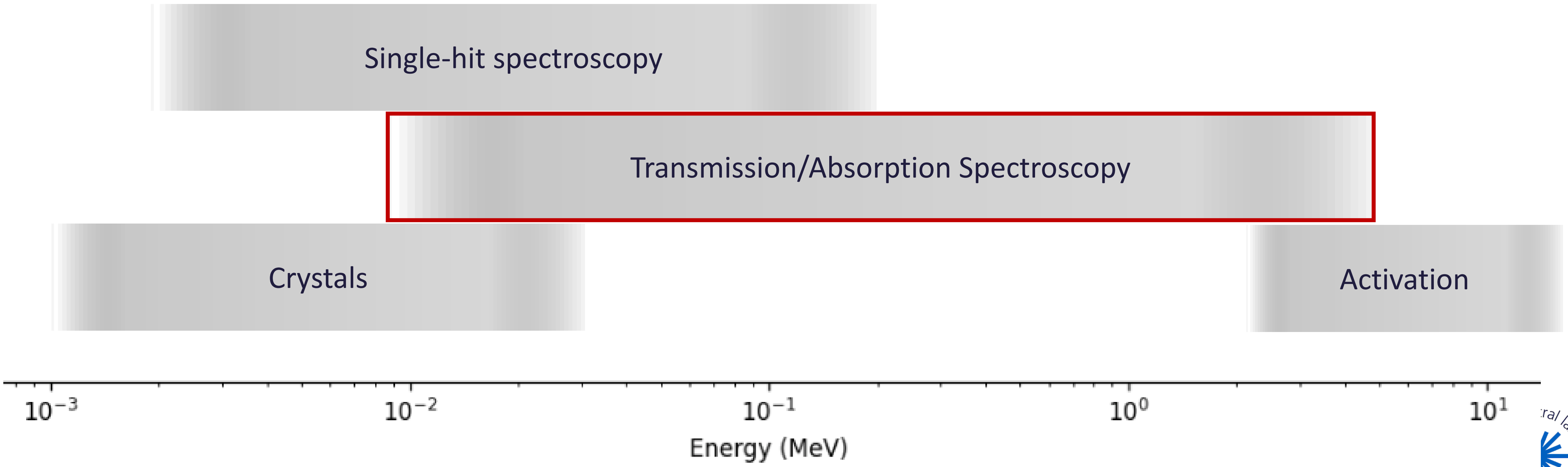

Chen, Rev. Sci. Instrum. 79, 10E305 (2008);

Absorption Spectrometers

Pass x-ray through a filter, measure response, pass through more of a filter, measure response.

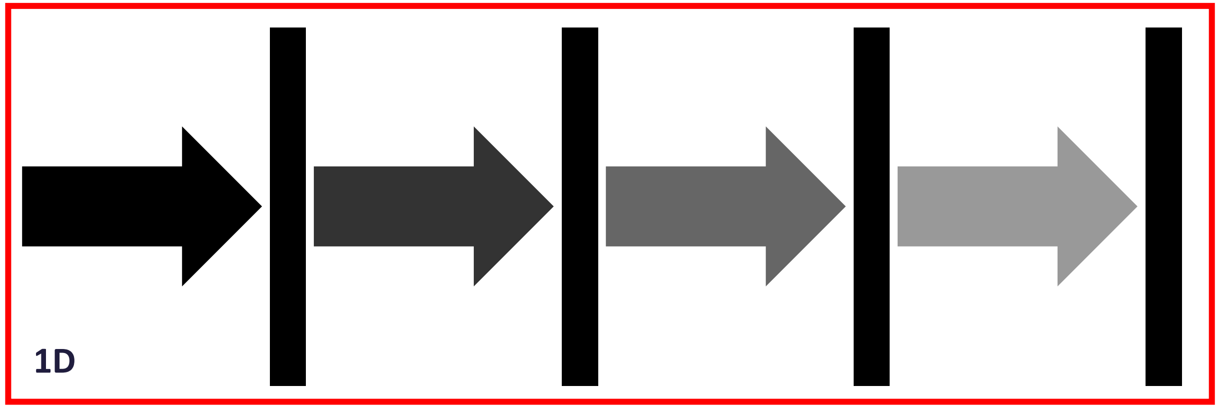

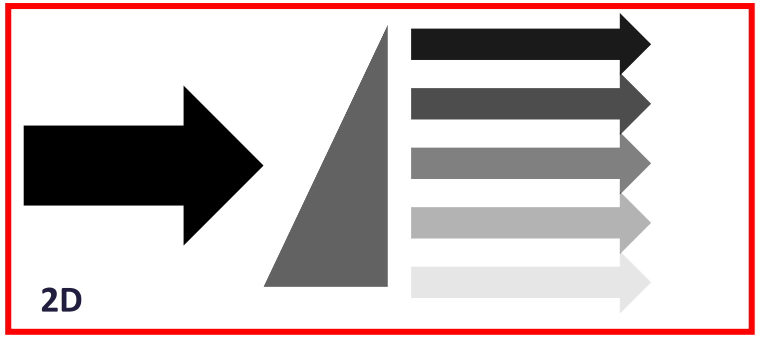

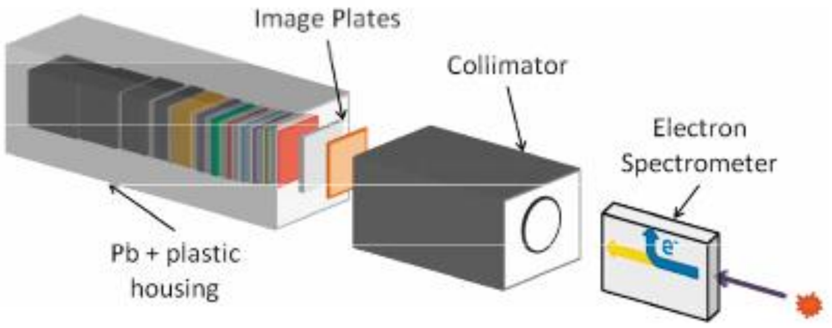

FIG. 1. (Color online) A diagram of the Bremsstrahlung spectrometer. The image plates are in a Lexan cartridge that fits into the Pb housing. The electron spectrometer deflects incident electrons.

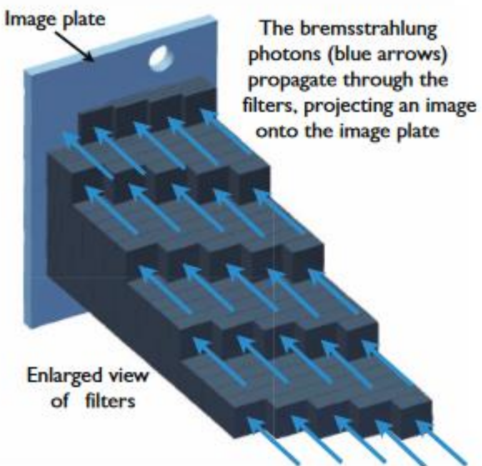

Scott, Rev. Sci. Instrum. 84, 083505 (2013);

FIG. 2. The incident bremsstrahlung photons (blue arrows) propagate through the filter array, creating an image on the region of image plate behind the filters, this image contains convolved information about the spectral distribution of the bremsstrahlung photons. The 25 filters create 25 energy bins.

Science and Technology Facilities Council

Reconstruction

In both cases reconstruction follows a form fitting process:

1. Define response of system
   - $R_k(E)$

2. Defined expected spectral form
   - $F(E, T_c)$

3. Scan parameters and compare to measured data
   - $\chi^2 = \sum_0^k \frac{(m_k - x_k)^2}{x_k}$
   - $x_k = R_k(E) \cdot F(E, T_C)$

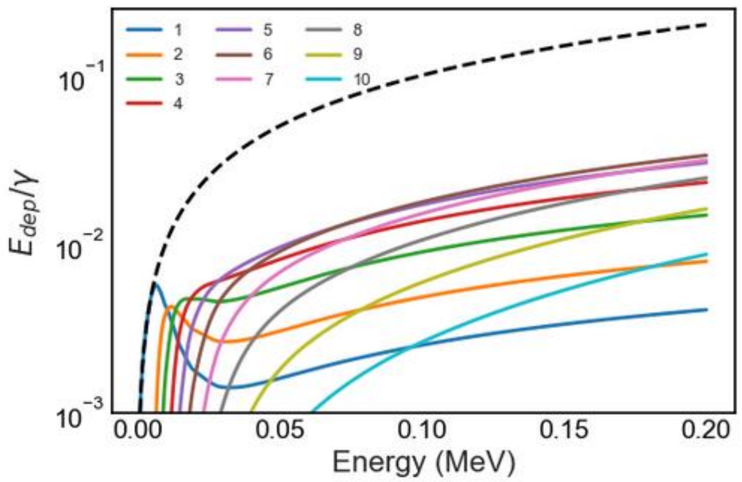

$$\frac{d^2 I_B}{d\Omega d\theta_B} = \frac{\gamma^2 \xi_B^2}{1 + \gamma^2 \theta_B^2} \left[K_{2/3}^2(\xi_B) + \frac{\gamma^2 \xi^2}{1 + \gamma^2 \theta_B^2} K_{1/3}^2(\xi_B) \right]$$

Parameter scan

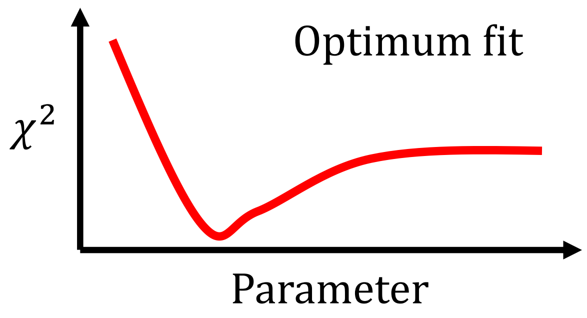

Science and Technology Facilities Council

Areal transmission spectroscopy

Element	Mo	Sn	Gd	Yb	Ag	Bi	Ag	Au	W	Zn	V
Thickness [μm]	50	50	50	50	40	40	20	10	25	5	3

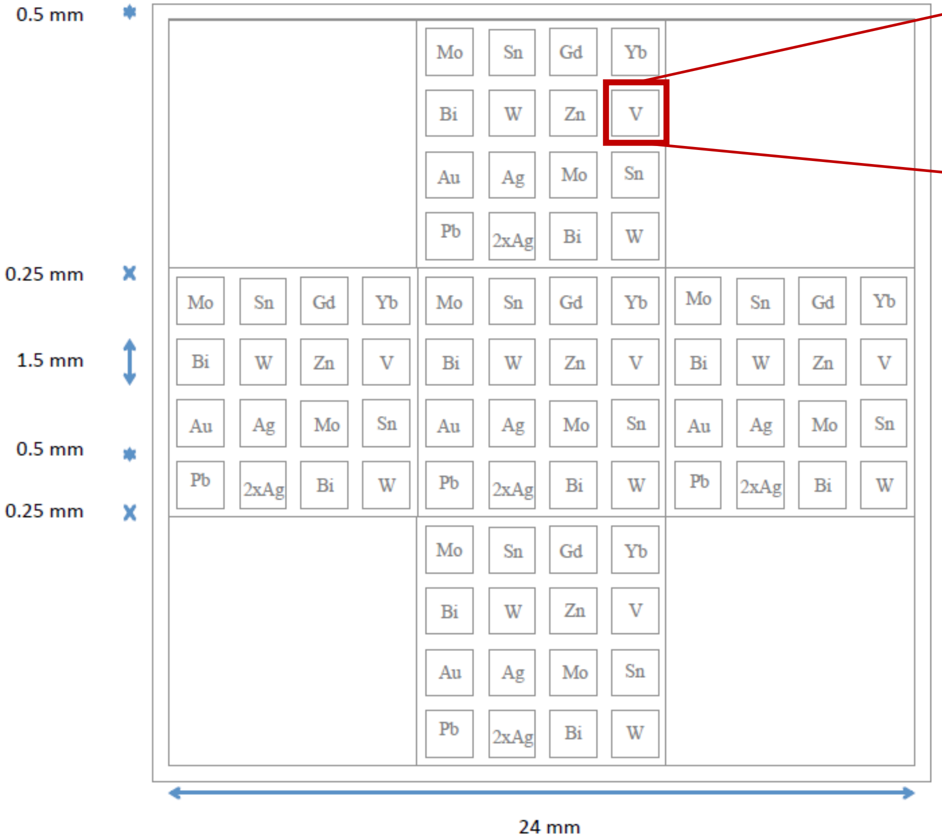

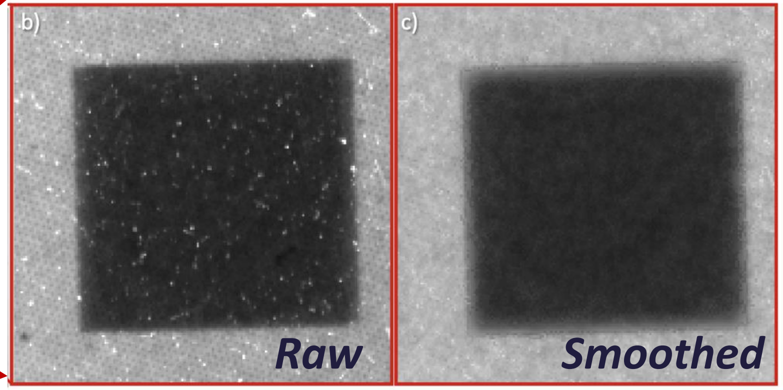

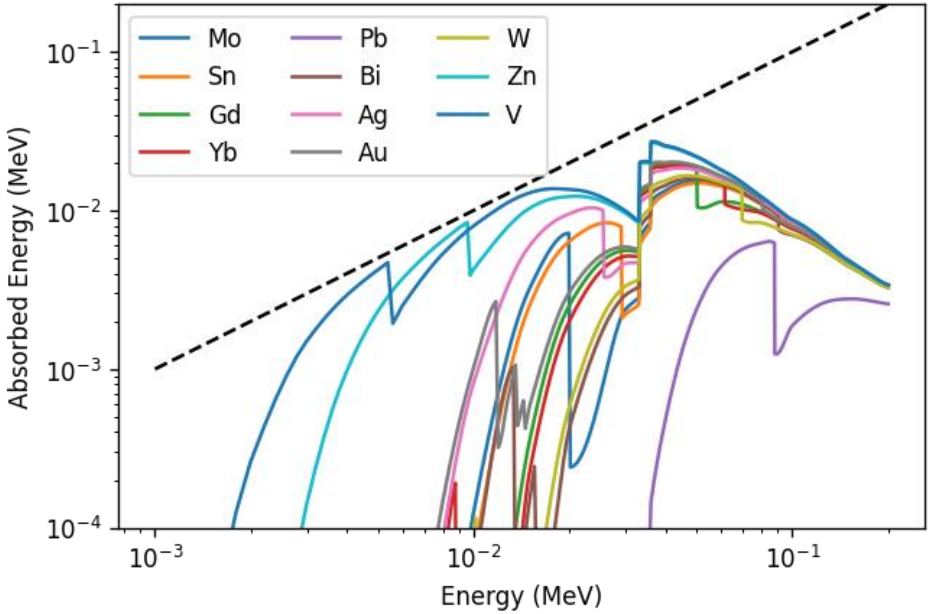

Technology Facilities Council

J. N. Gruse, *Development of laser wakefield accelerators*. Diss. Imperial College London, (2020)

Areal transmission spectroscopy

Element	Mo	Sn	Gd	Yb	Ag	Bi	Ag	Au	W	Zn	V
Thickness [μm]	50	50	50	50	40	40	20	10	25	5	3

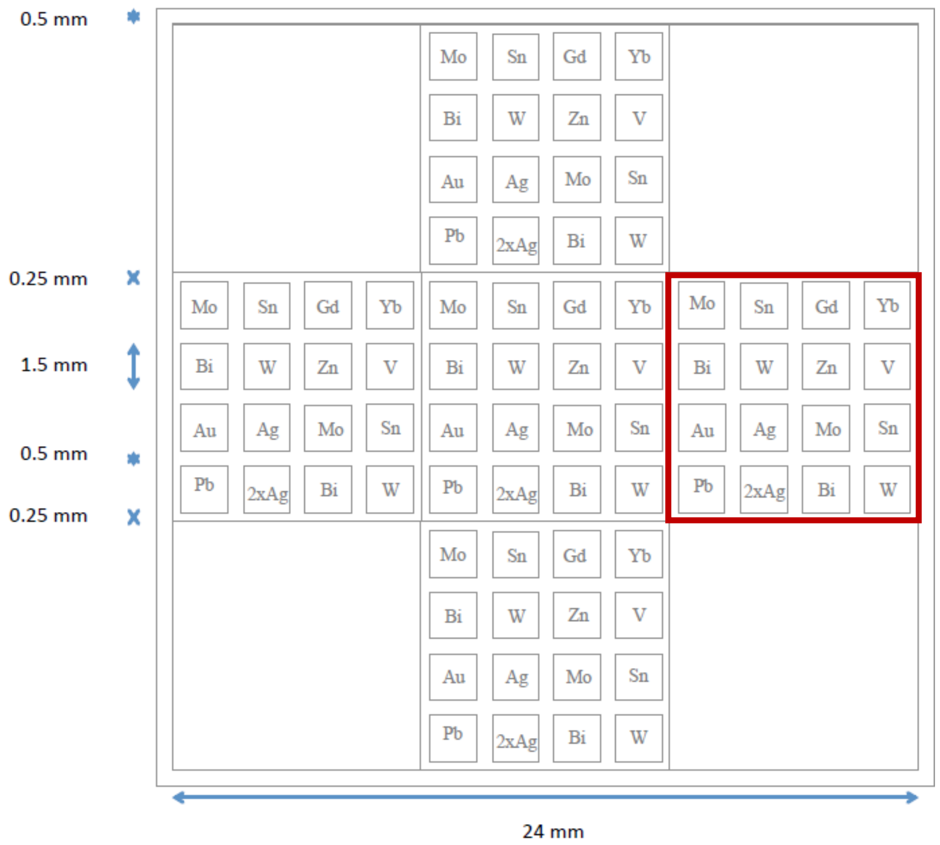

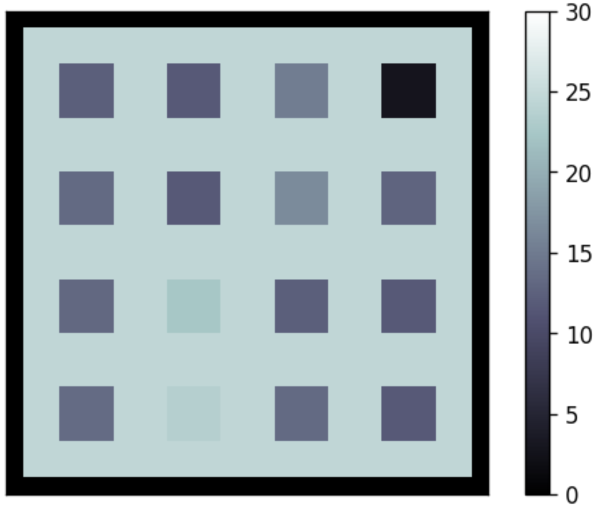

Synth output from grid

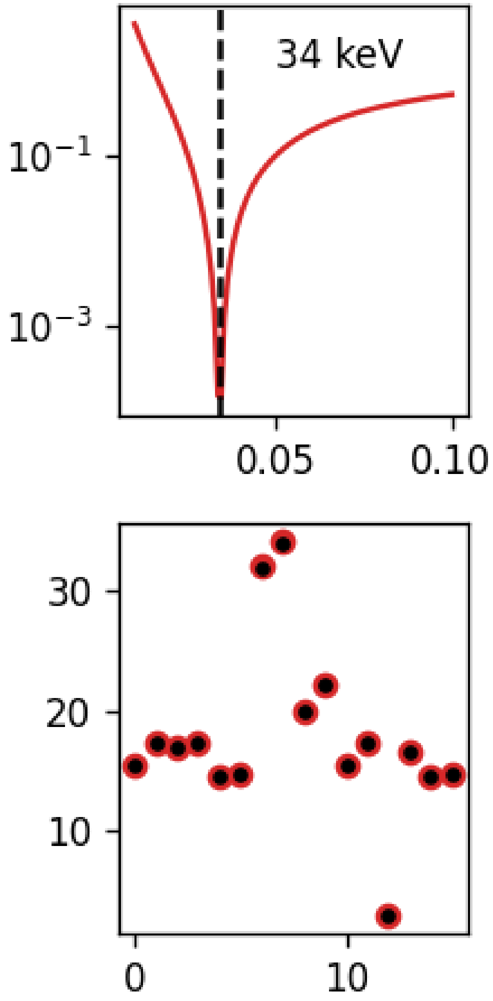

Science and Technology Facilities Council

Ross-pair transmission spectroscopy

Matching similar transmission functions with different elements provides an *effective* delta function from which we can isolate different spectral combinations.

We still require the beam to be spatially uniform in each region but we can define smaller masks to sample the area at multiple points.

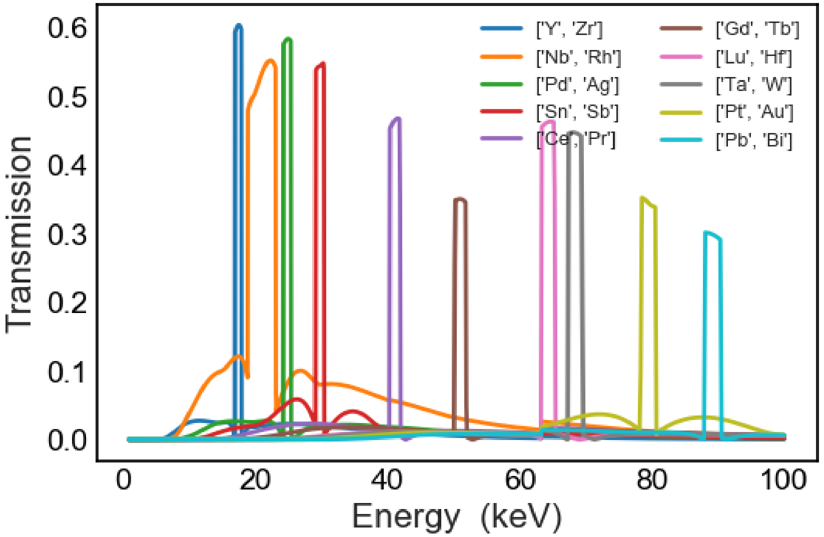

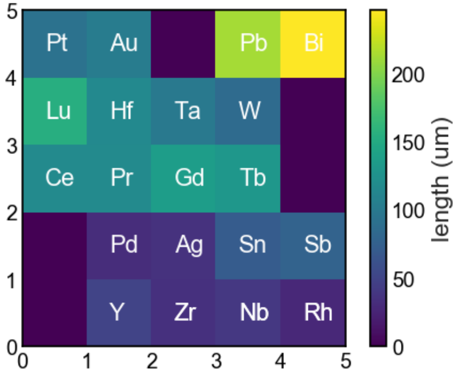

$$nE_k \approx \kappa\eta\left[\int_0^\infty f(E)\mathrm{e}^{-\sigma_1\rho_1\ell_1}dE - \int_0^\infty f(E)\mathrm{e}^{-\sigma_2\rho_2\ell_3}dE\right]$$

$$nE_k \approx \frac{I_1 - I_2}{\kappa\eta}$$

Science and Technology Facilities Council

Linear absorption spectroscopy

Similar idea as before but each layer is also a detector plane, and since this samples a ~1D point we don't need to assume a uniform spectro-spatial distribution

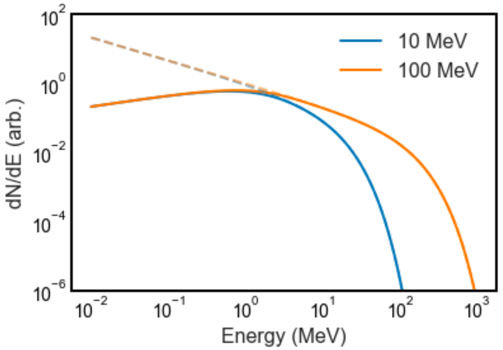

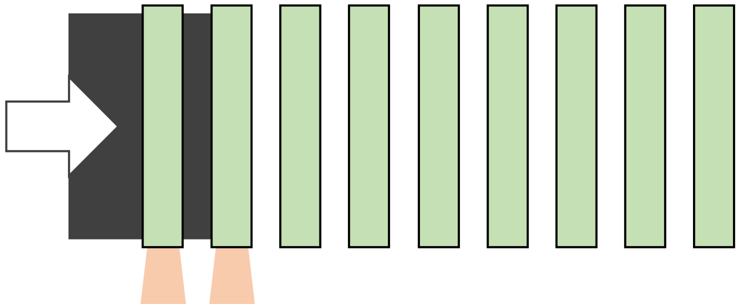

Rusby, D.R. *et al* Rev. Sci. Instrum.89, 073502 (2018)

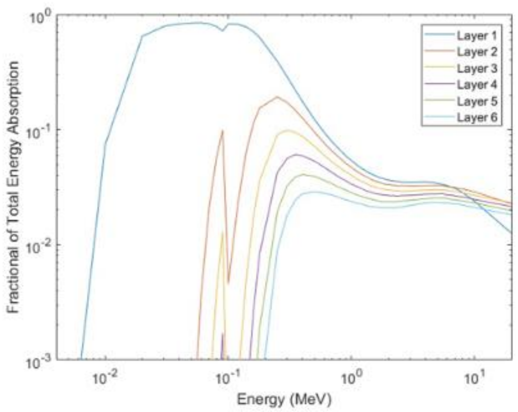

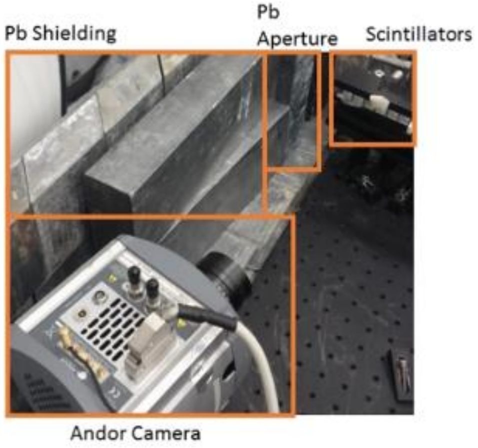

Chen, Rev. Sci. Instrum. 79, 10E305 (2008);

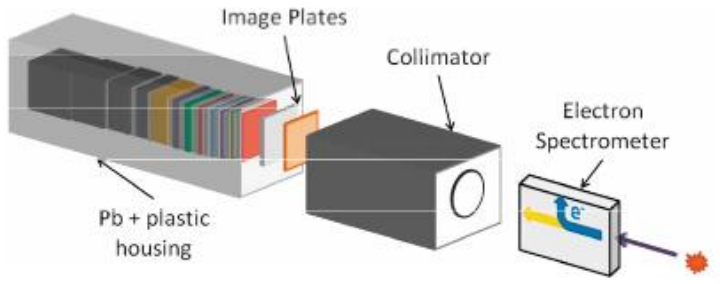

FIG. 1. (Color online) A diagram of the Bremsstrahlung spectrometer. The image plates are in a Lexan cartridge that fits into the Pb housing. The electron spectrometer deflects incident electrons.

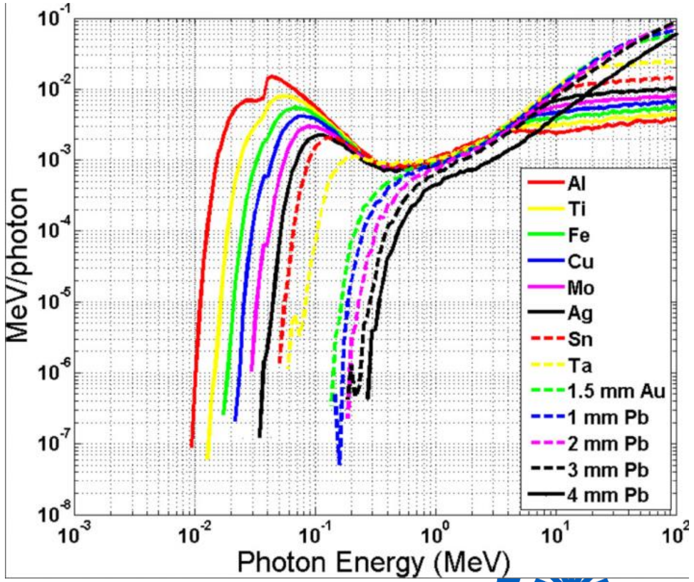

Science and Technology Facilities Council

Reconstruction

$$\Gamma * F = M$$

From the response matrix expected responses for a series of incident spectra can be determined.

$$\begin{bmatrix} R_{L_1,E_1} & R_{L_1,E_N} \\ \cdots & \cdots \\ R_{L_N,E_1} & R_{L_N,E_N} \end{bmatrix} * \begin{bmatrix} F_{E_1} \\ \cdots \\ F_{E_N} \end{bmatrix} = \begin{bmatrix} M_1 \\ \cdots \\ M_N \end{bmatrix}$$

$$\Gamma(E) \quad * \quad F(E) \quad = \quad \langle M \rangle$$

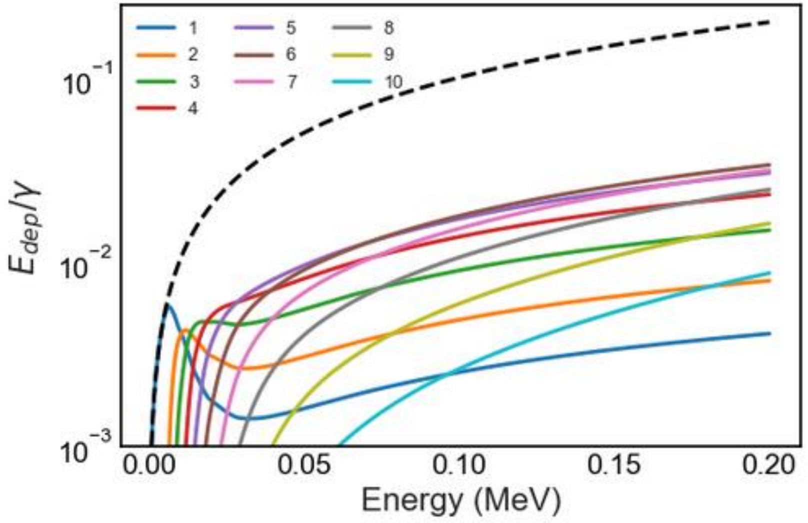

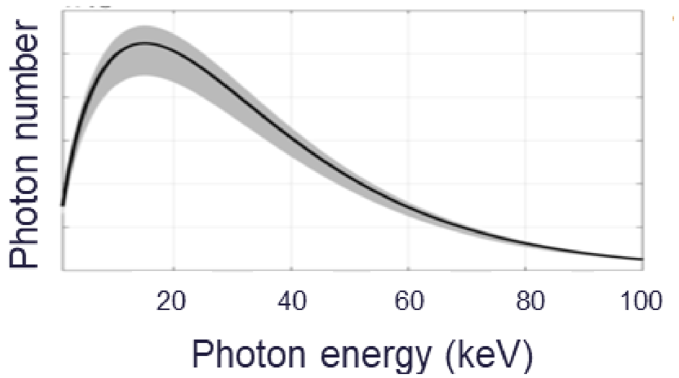

$$\frac{d^2 I_B}{d\Omega d\theta_B} = \frac{\gamma^2 \xi_B^2}{1+\gamma^2\theta_B^2}\left[K_{2/3}^2(\xi_B) + \frac{\gamma^2 \xi^2}{1+\gamma^2\theta_B^2} K_{1/3}^2(\xi_B)\right]$$

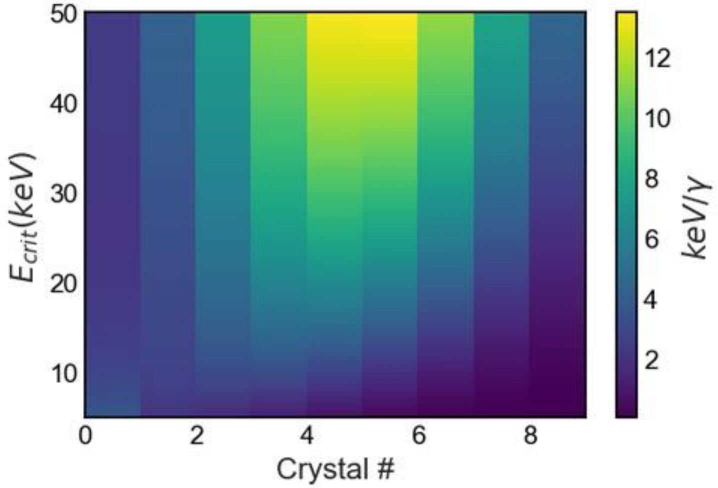

Science and Technology Facilities Council

Reconstruction

Consider a standard betatron arrangement:

- LWFA produces e^- and γ_β
- Remaining laser is dumped on flange/tape drive
- e^- is not immediately swept clear interacts with beam dump and produces a secondary burst of γ_k

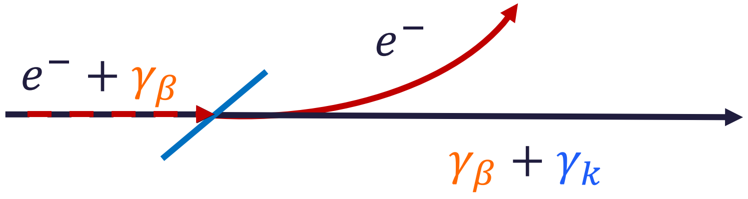

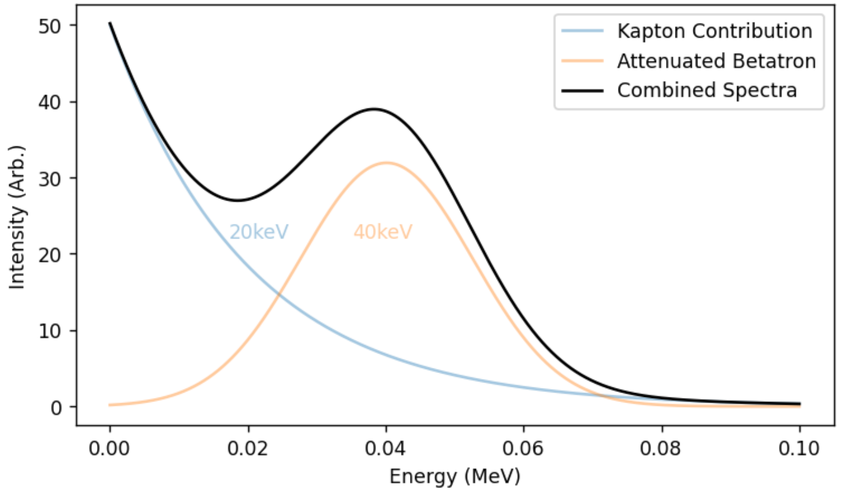

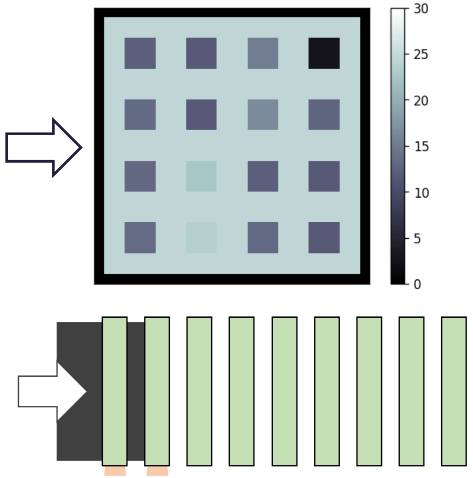

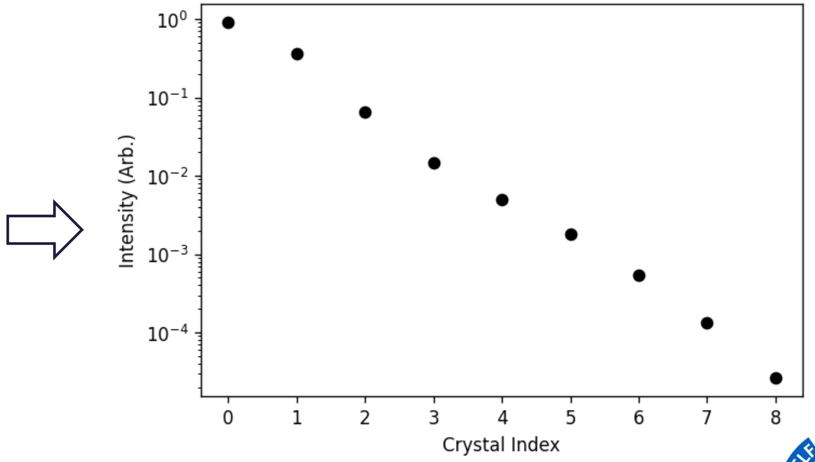

Technology Facilities Council

central laser facility

Reconstruction

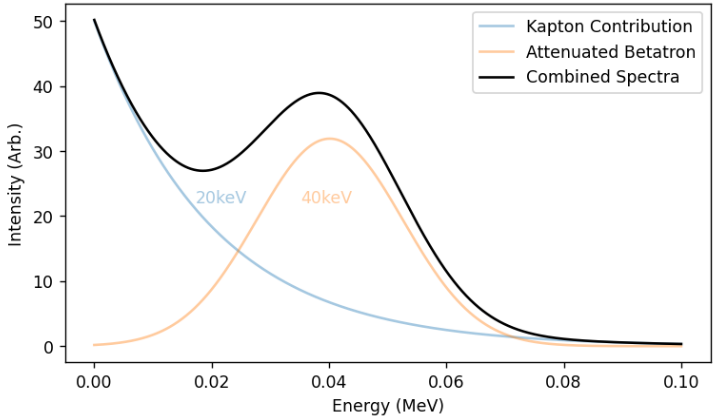

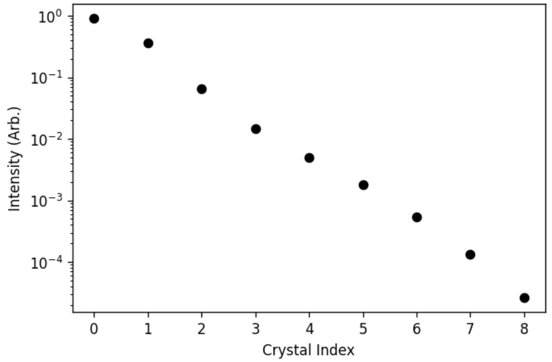

Piecewise 1D Scan

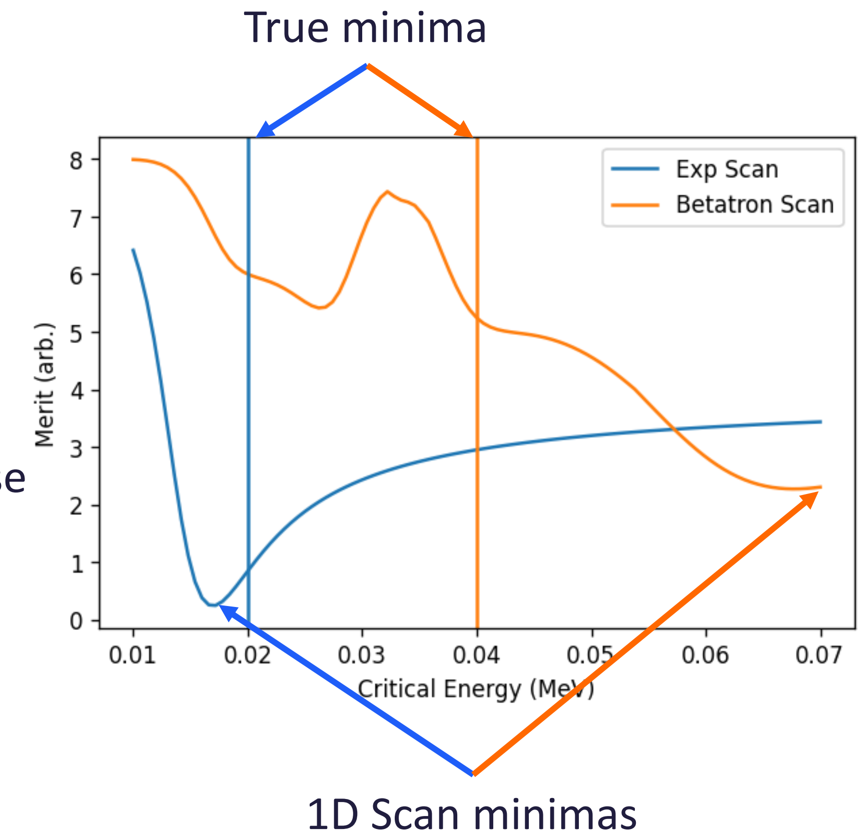

Scanning the parameter space scales with number of parameters.

*By only 3 parameters this could already **impact Hz** level operation*

Scanning Parameter Space

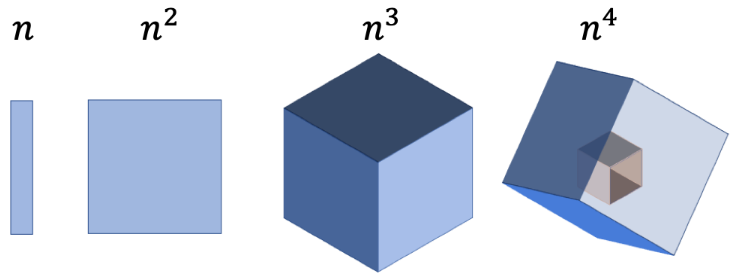

	n	n^2	n^3	n^4
Parameters to check	100	10000	1000000	100000000
Time to compute (1us per comparison)	<ms	..at 100 Hz	..a second	..over a minute

Treating these systems independently we cannot find the ground truth! And the problem is that we still achieve a good merit function!

Instead, we have to solve for both components simultaneously!

Science and Technology Facilities Council

Reconstruction

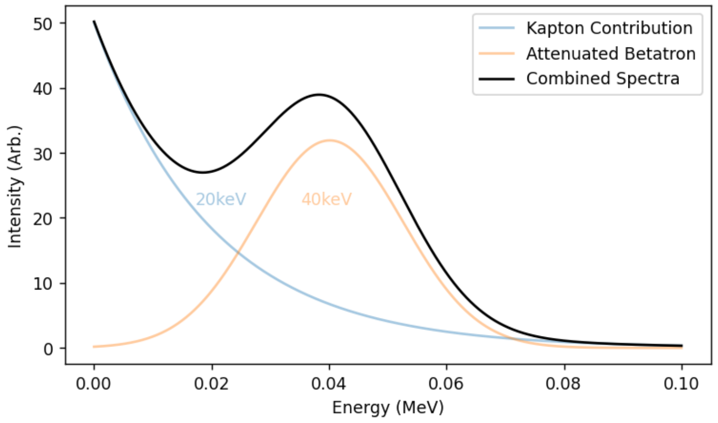

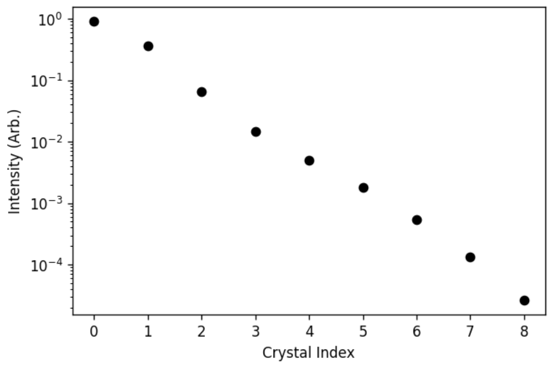

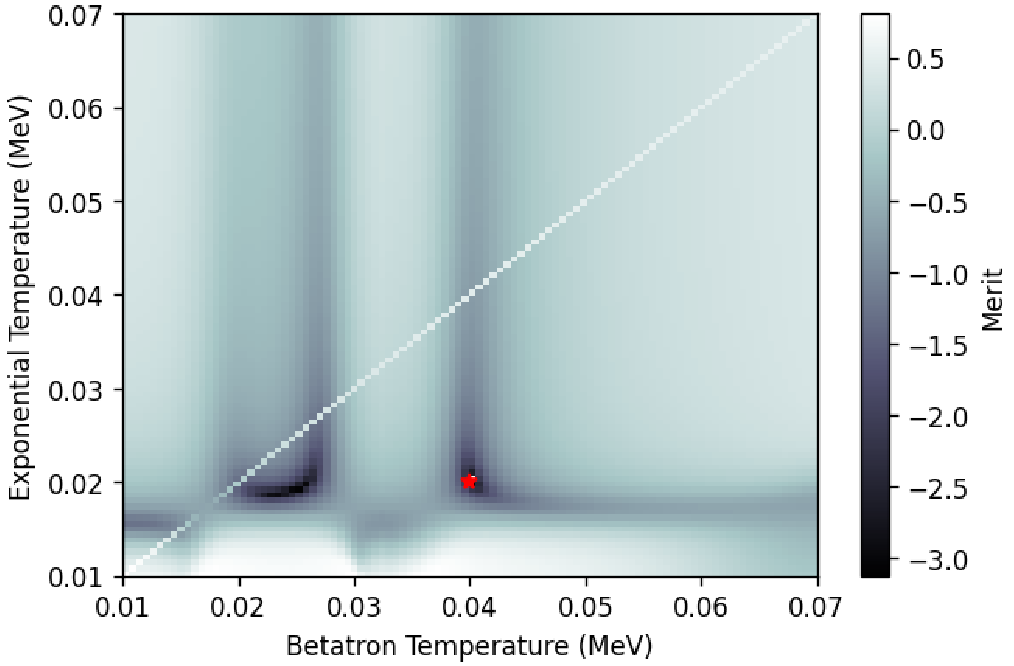

Brute force grid-scan

- **4x unknown dimensions to scan**
- **2x temperatures (1x exponential, 1x betatron)**
- **2x fluxes (1x exponential, 1x betatron)**

Scanning 100 values for each parameter = 10^8 sets to check!

Analytical flux reduction

- **2x temperatures to scan**
- **2x fluxes to solve for**

Scanning 100 values for each parameter = 10^4 sets to check!

Science and Technology Facilities Council

central laser facility

C. D. Armstrong, *et al.* RSI 92 (**11**): 113102 (2021)
https://doi.org/10.1063/5.0057486

Reconstruction

Multiple components combine for our measured signal as:

$$S_k = n_1 \int_0^\infty f_1(E_\gamma, T_1)\Gamma(k, E_\gamma)dE_\gamma + n_2 \int_0^\infty f_2(E_\gamma, T_2)\Gamma(k, E_\gamma)dE_\gamma + \cdots ,$$

We wish to then find the sum of spectral terms that most closely matches the measured data M_k:

$$\delta = 1 - \frac{n_1 R_1}{M_k} - \frac{n_2 R_2}{M_k} \ldots$$

$$Q \cdot R_1 = [n_1 R_1 - n_2 R_2 \ldots] \cdot R_1$$
$$Q \cdot R_2 = [n_1 R_1 - n_2 R_2 \ldots] \cdot R_2$$
$$\ldots$$
$$Q \cdot R_n = [n_1 R_1 - n_2 R_2 \ldots] \cdot R_n$$

1- Component

$$n_1 = \frac{QR_1}{R_{11}}.$$

2- Component

$$n_1 = \frac{QR_2R_{12} - QR_1R_{22}}{R_{12}^2 - R_{11}R_{22}},$$
$$n_2 = \frac{-QR_2R_{11} + QR_1R_{12}}{R_{12}^2 - R_{11}R_{22}}.$$

3-Component

$$n_1 = \frac{QR_3R_{13}R_{22} - QR_3R_{12}R_{23} - QR_2R_{13}R_{23} + QR_1R_{23}^2 + QR_2R_{12}R_{33} - QR_1R_{22}R_{33}}{R_{13}^2R_{22} - 2R_{12}R_{13}R_{23} + R_{11}R_{23}^2 + R_{12}^2R_{33} - R_{11}R_{22}R_{33}},$$
$$n_2 = \frac{-QR_3R_{12}R_{13} + QR_2R_{13}^2 + QR_3R_{11}R_{23} - QR_1R_{13}R_{23} - QR_2R_{11}R_{33} + QR_1R_{12}R_{33}}{R_{13}^2R_{22} - 2R_{12}R_{13}R_{23} + R_{11}R_{23}^2 + R_{12}^2R_{33} - R_{11}R_{22}R_{33}},$$
$$n_3 = \frac{QR_3R_{12}^2 - QR_2R_{12}R_{13} - QR_3R_{11}R_{22} + QR_1R_{13}R_{22} + QR_2R_{11}R_{23} - QR_1R_{12}R_{23}}{R_{13}^2R_{22} - 2R_{12}R_{13}R_{23} + R_{11}R_{23}^2 + R_{12}^2R_{33} - R_{11}R_{22}R_{33}}.$$

Science and Technology Facilities Council

Science and Technology Facilities Council

Spectral Characterisation

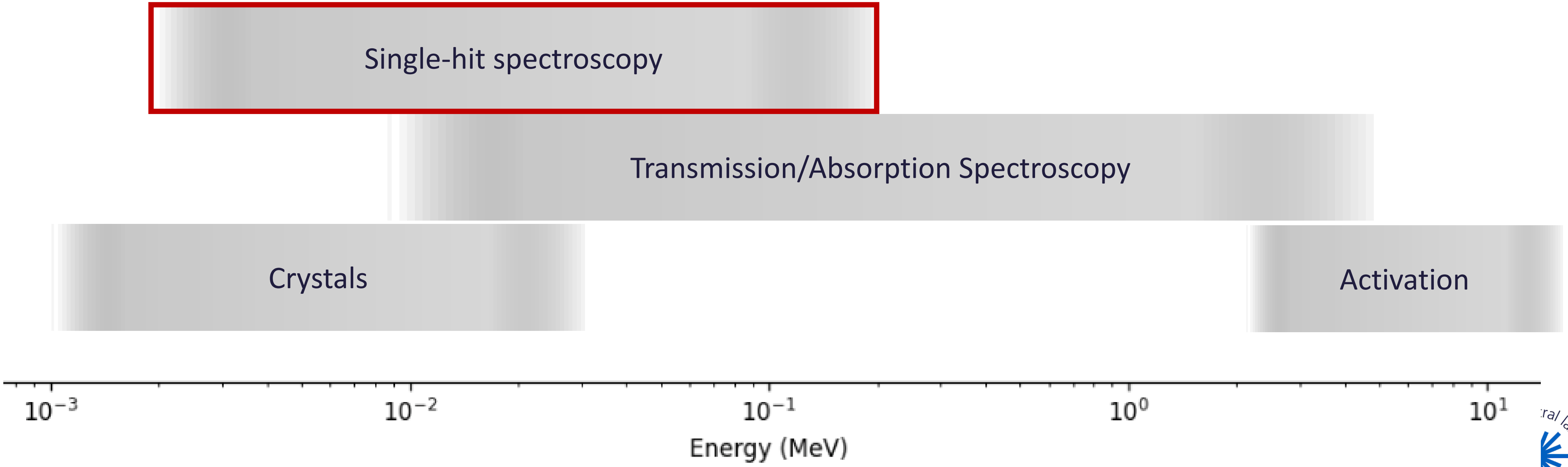

Single-hit spectroscopy

X-ray photon comes in, electrons are freed proportional to the energy deposited. More energy deposited -> more electrons.

If we count all the electrons we can say how much energy arrived.

Same assumptions to the absorption spectrometers before but now we don’t need to consider the spectral shape.

Requires two things:

- 1 photon per *measurement*
- Calibrated, ideally linear, energy resolving detector

Works as either scintillators or semiconductors with benefits to each design.

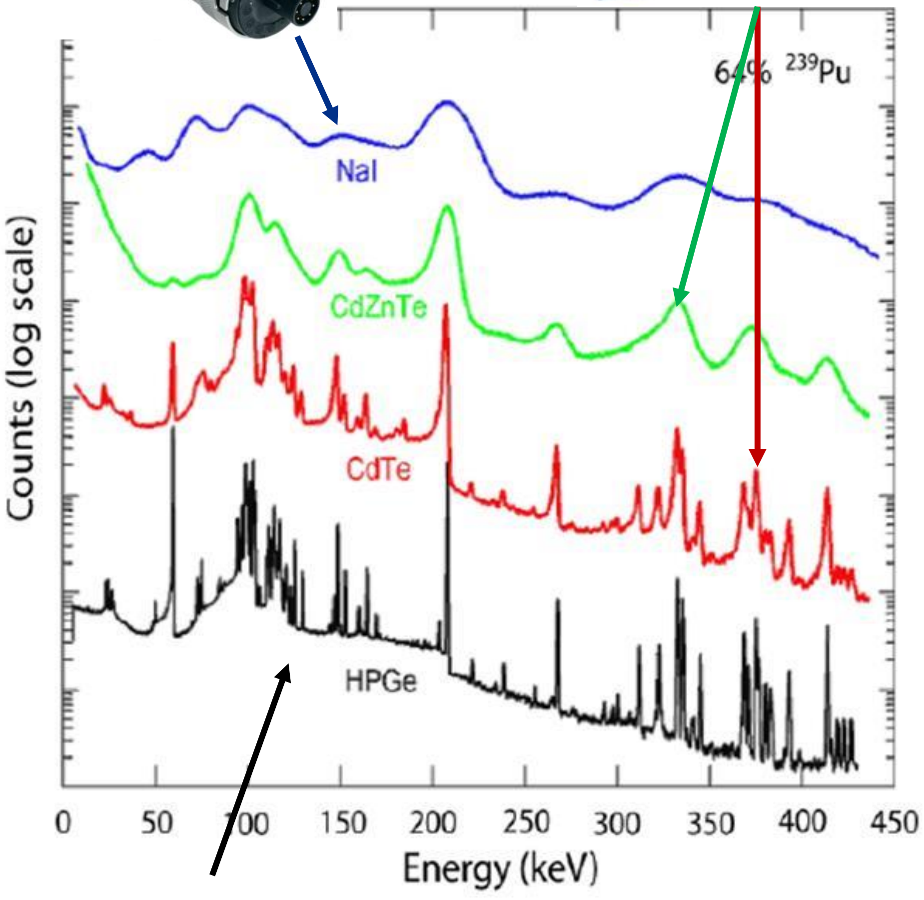

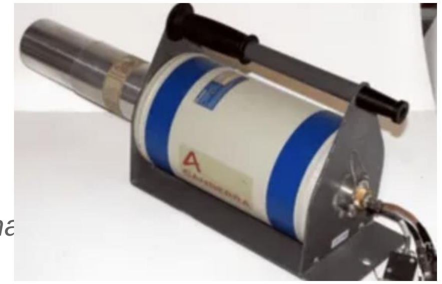

Science and Technology Facilities Council

Single-hit spectroscopy

Requires two things:

- 1 photon per *measurement*
- Calibrated, ideally linear, energy resolving detector

To at least approach a single shot characterisation we need to think about the number of measurements we can acquire.

There are two factors at play;

- the ***number of samples per frame***,
- the ***number of frames per pulse***.

Science and Technology Facilities Council

central laser facility

Single-hit spectroscopy

Requires two things:

- 1 photon per *measurement*
- Calibrated, ideally linear, energy resolving detector

To at least approach a single shot characterisation we need to think about the number of measurements we can acquire.

There are two factors at play;

- the ***number of samples per frame***,
- the ***number of frames per pulse***.

Source

$\int f(t)dt = c$

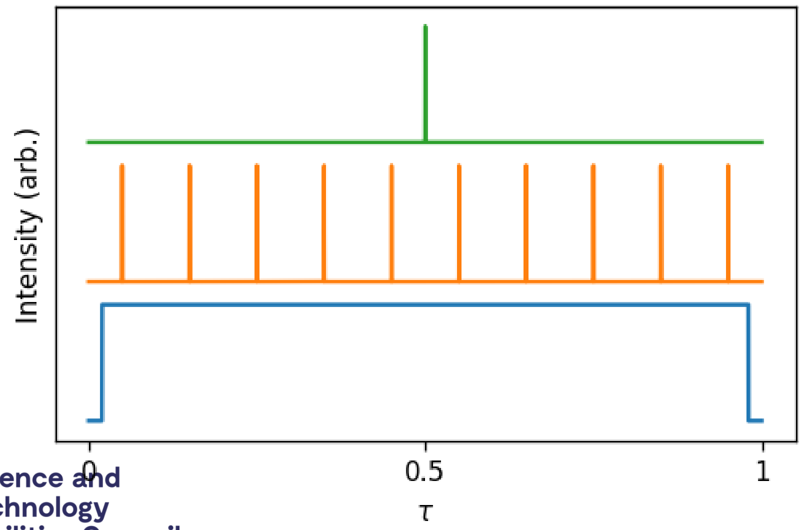

Sampling

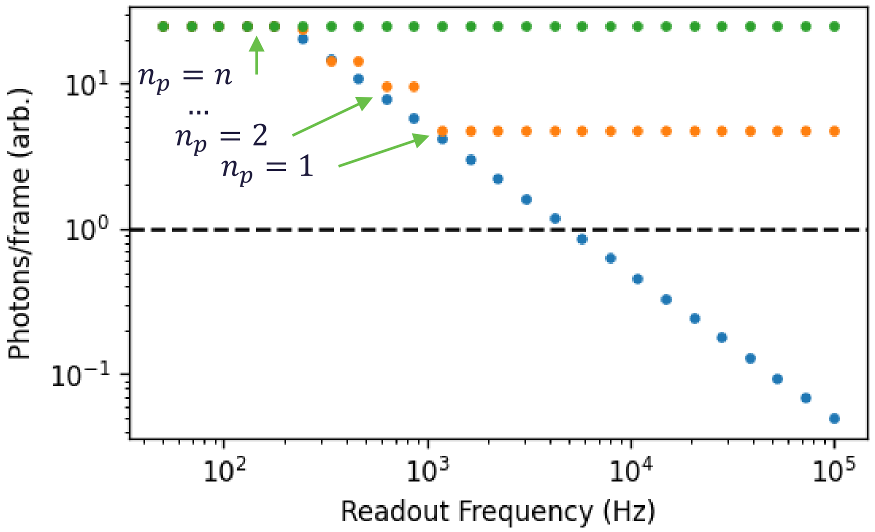

Science and Technology Facilities Council

Single-hit spectroscopy

To increase the number of samples per frame without requiring frequencies below the pulse duration of the laser **(~PHz)** we can instead increase the number of channels or pixels.

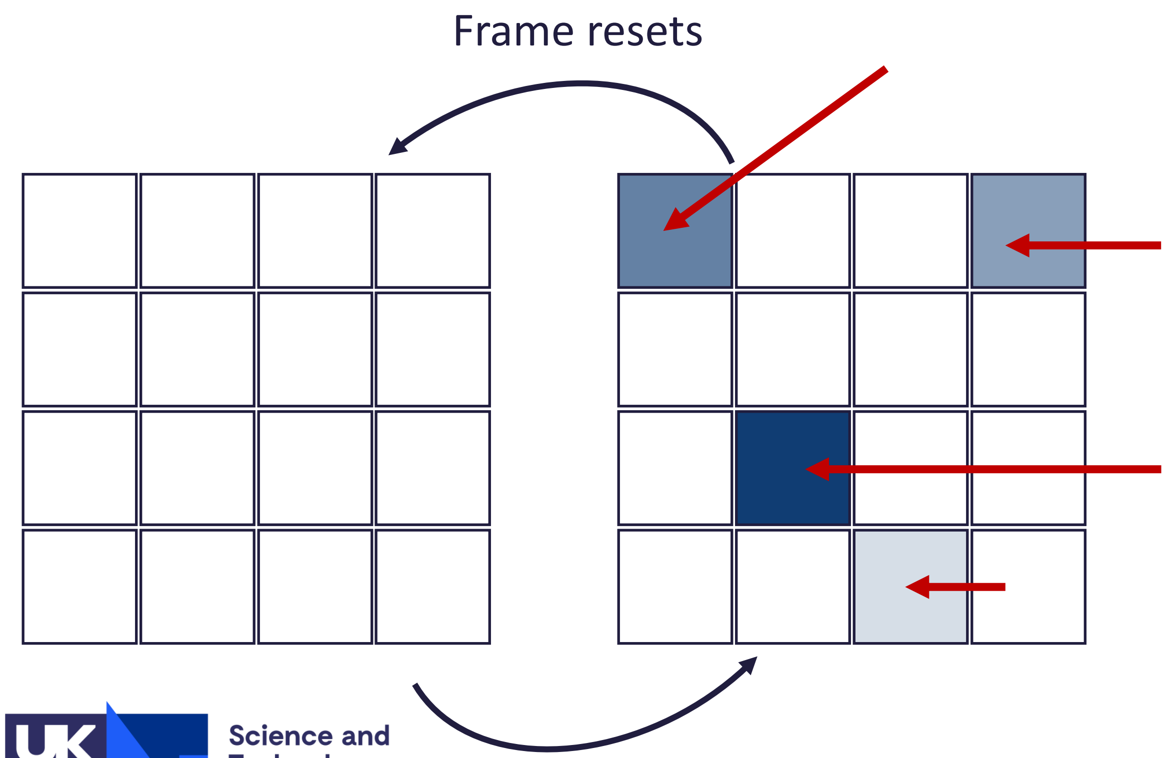

In doing so we move the number of events per frame we can accept

For ***laser driven sources*** we combined this with divergence of the beam and r^2 (reducing the number of photons arriving per pixel)

Single-hit spectroscopy

To increase the number of samples per frame without requiring frequencies below the pulse duration of the laser **(~PHz)** we can instead increase the number of channels or pixels.

CPU Frequency World Record ranking on 17 August 2023

RANK	SCORE	USER	PROCESSOR
#1	9008.82 MHz	elmor	Intel Core i9 13900K (8P) @ 9008.8MHz
#2	8725.49 MHz	SuperO	Intel Core i9 13900K (8P) @ 8725.5MHz
#3	8722.78 MHz	The Stilt	AMD FX-8370 @ 8722.8MHz
#4	8716 MHz	safedisk	Intel Core i9 13900K (8P) @ 8716MHz
#5	8709 MHz	AndreYang	AMD FX-8150 @ 8709MHz

100x faster *than the current record CPU …*

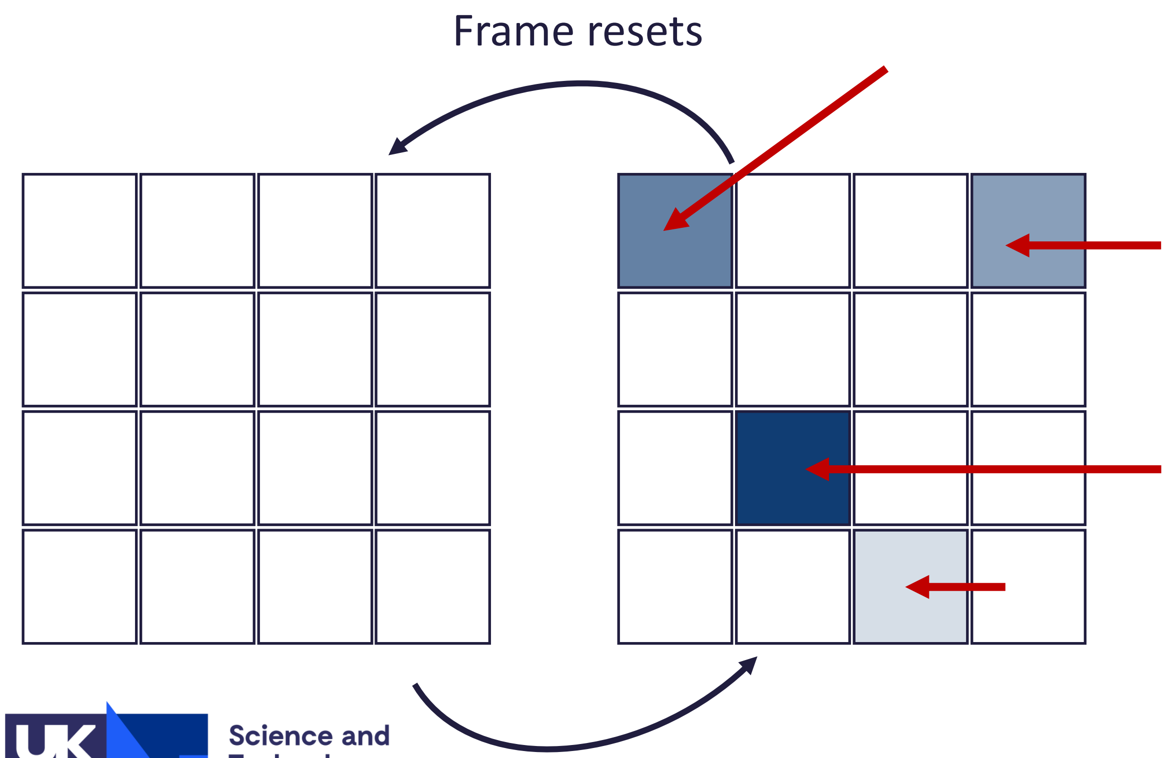

In doing so we move the number of events per frame we can accept

For ***laser driven sources*** we combined this with divergence of the beam and r^2 (reducing the number of photons arriving per pixel)

Overcoming Occupancy

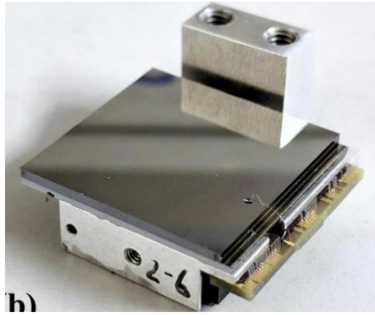

Single sensor:

80 x 80 pixels at 250um pitch: 6400px
~640 samples per shot at maximum density

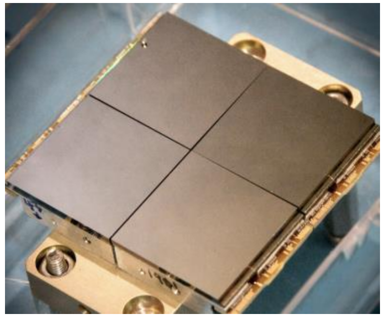

2x2 sensor:

25kpx
~2500 samples per shot at maximum density

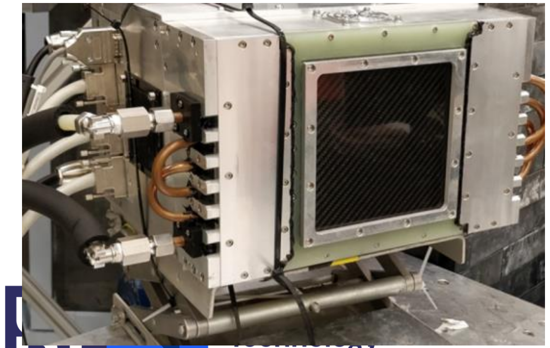

5x5 sensor:

160kpx
~16000 samples per shot at maximum density

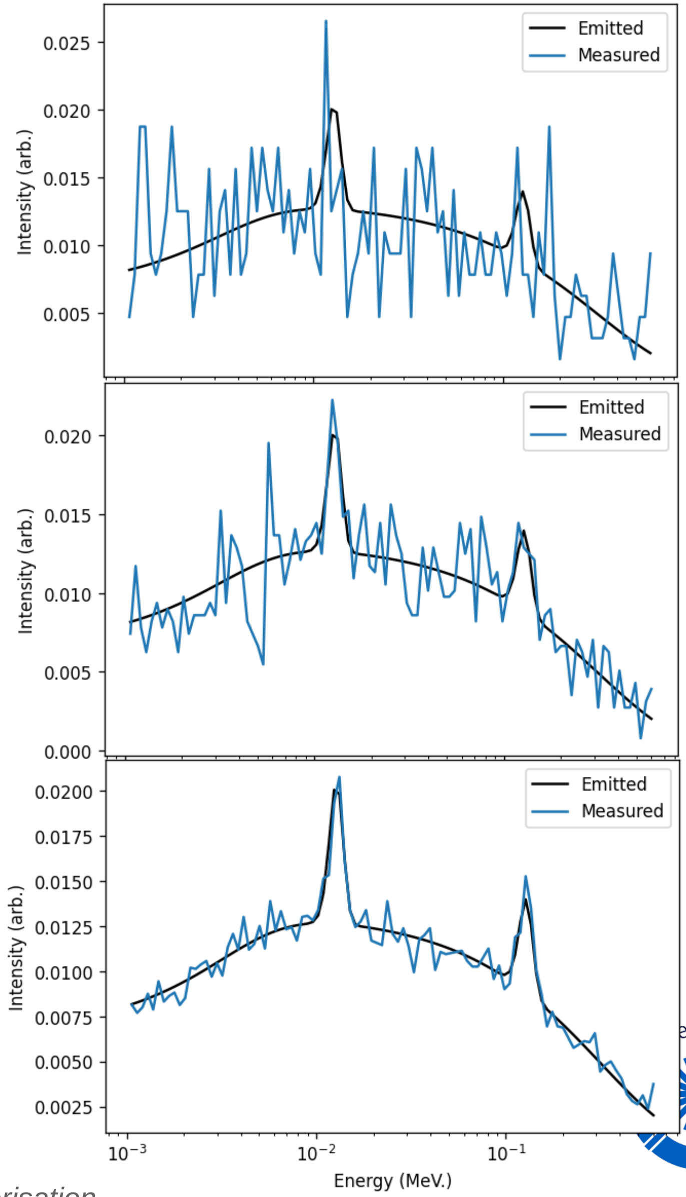

Facilities Council

Science and Technology Facilities Council

Spatial Characterisation

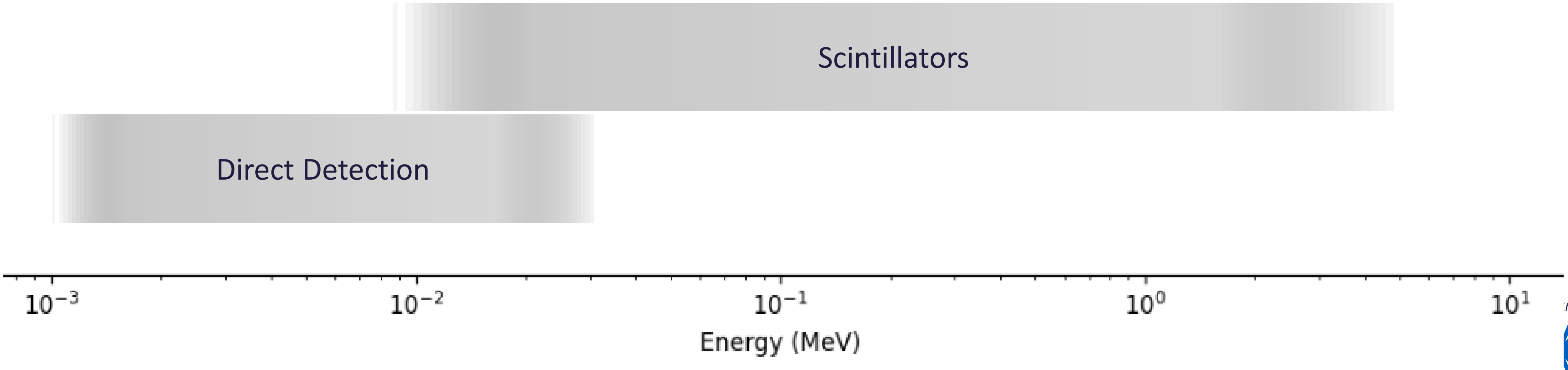

Spatial Characterisation

As with spectral characterisation there are two main detectors schemes, either direct detection or indirect (via a scintillator):

Direct detectors

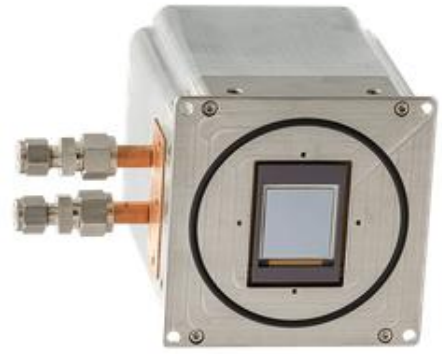

Indirect detectors

Contact/FOP Scintillators

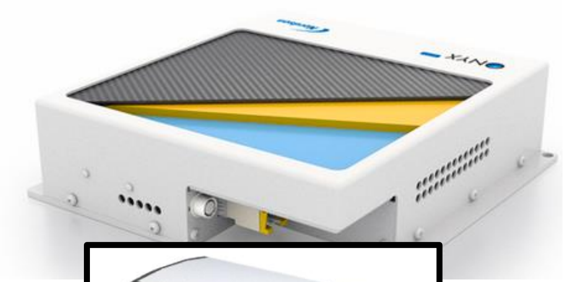

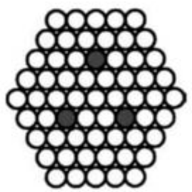

Fig.5: Statistical EMA

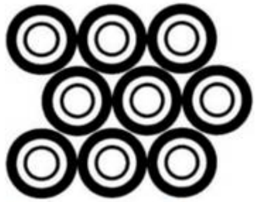

Fig.6: Annular EMA

Lens based scintillators

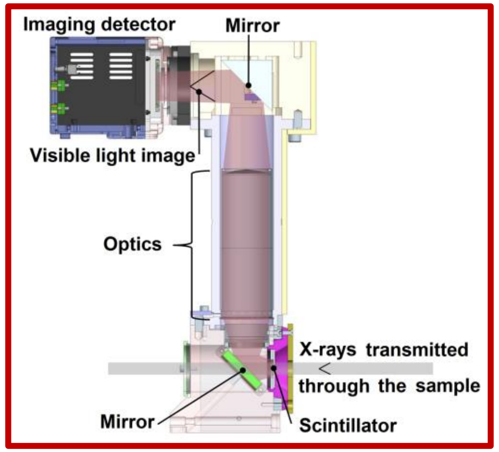

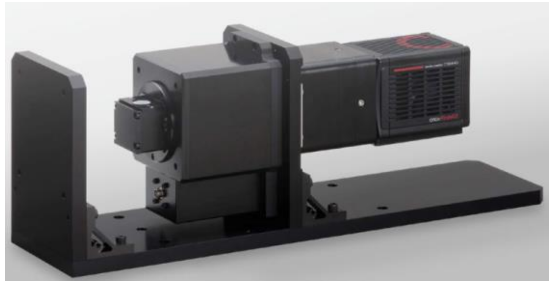

Science and Technology Facilities Council

central laser facility

"...resolution was detector limited"

Inline – Direct Coupling

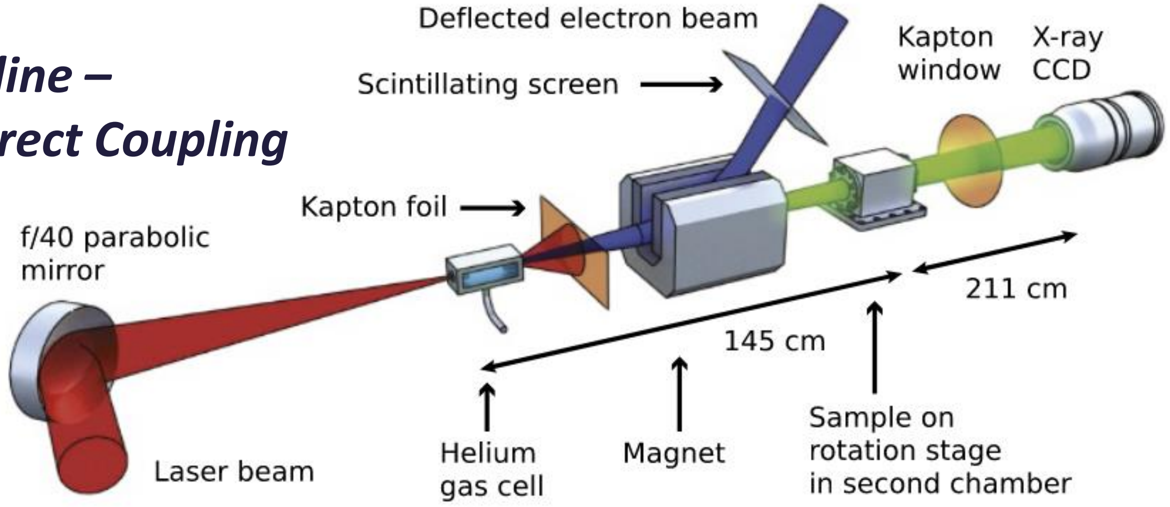

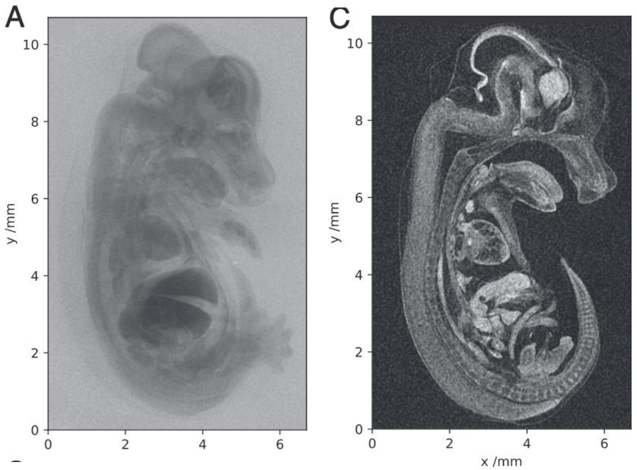

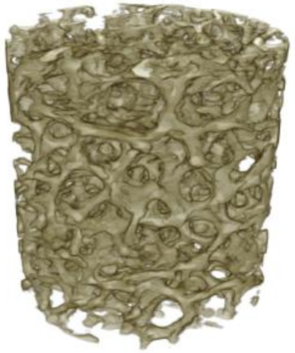

High opacity

Offline – Lens Coupling

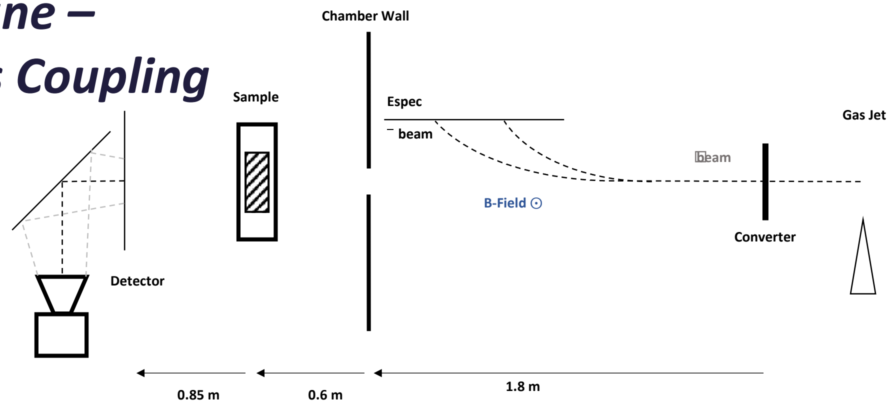

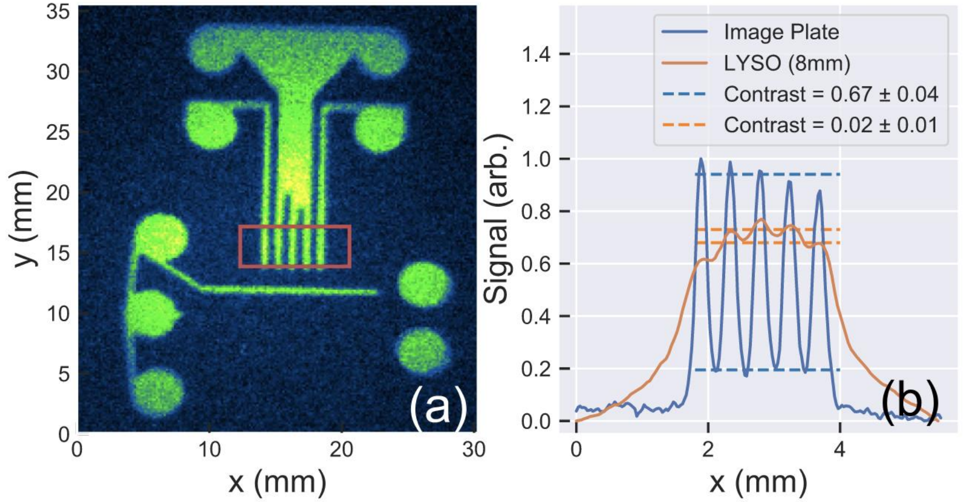

Science and Technology Facilities Council

central laser facility

"...resolution was detector limited"

Inline – Direct Coupling

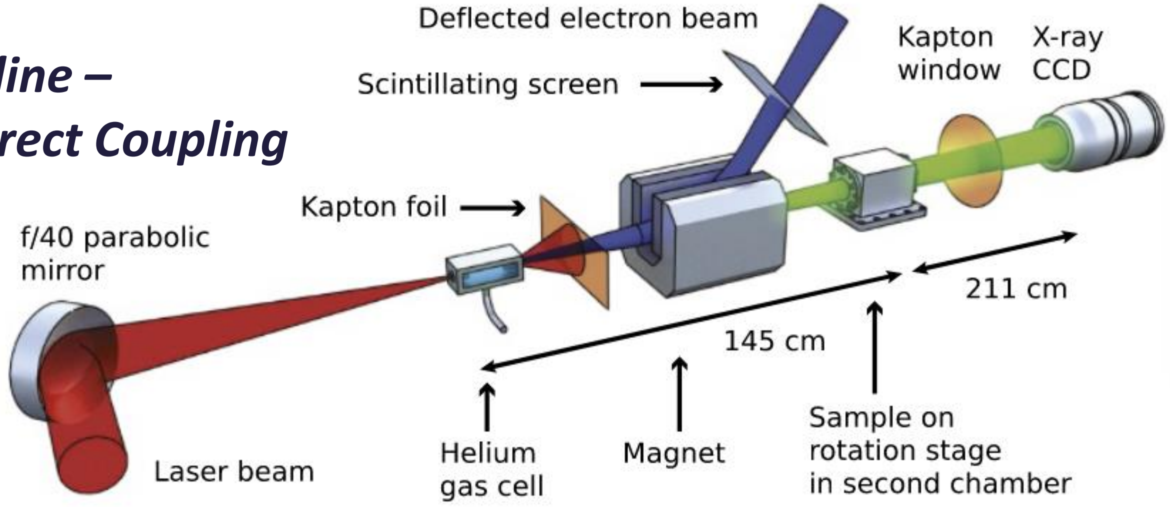

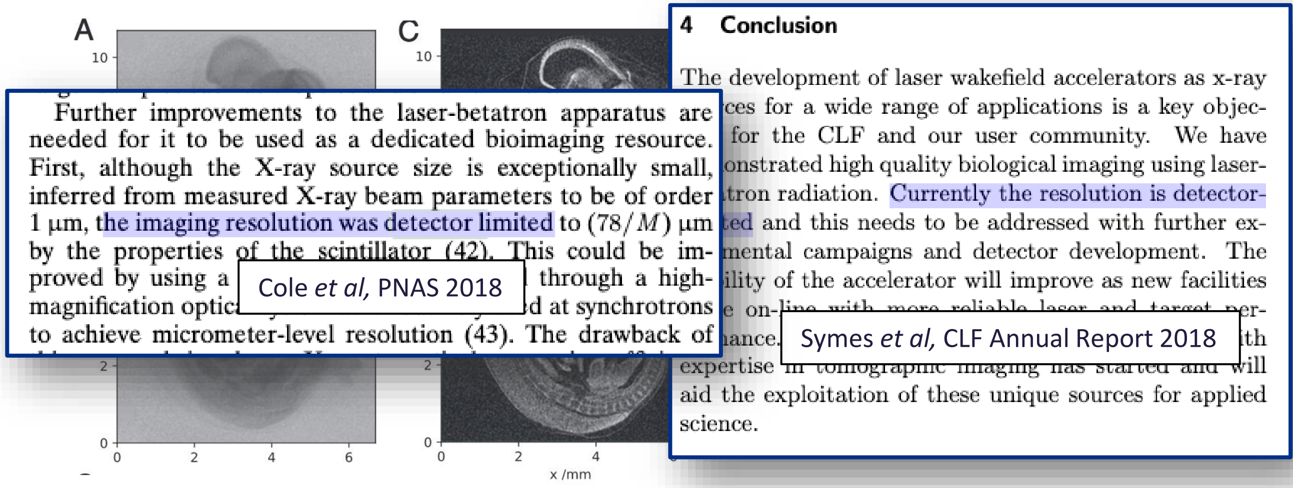

Offline – Lens Coupling

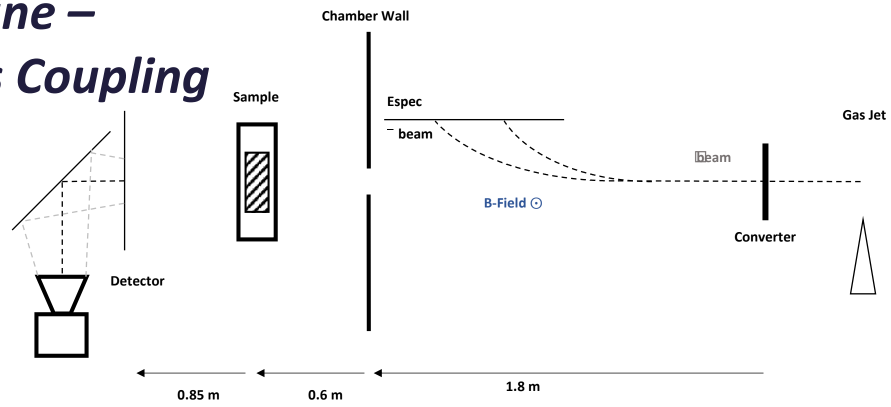

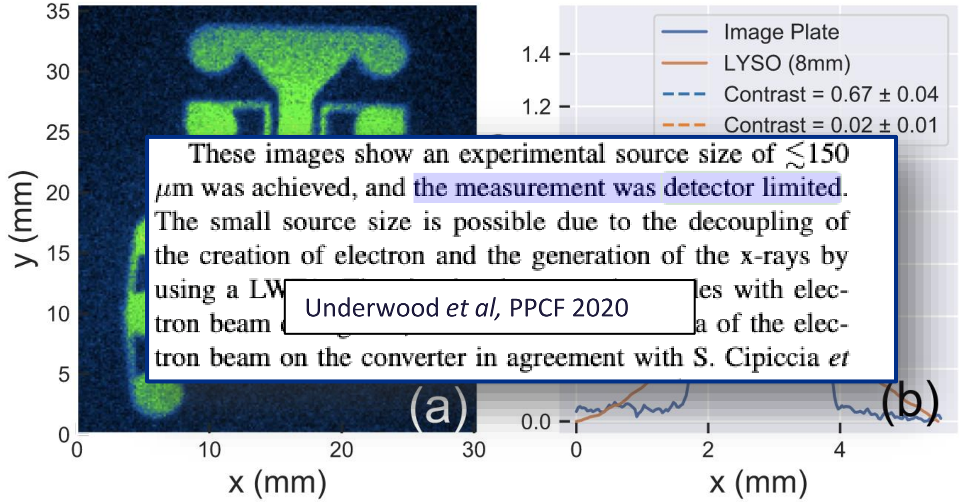

Science and Technology Facilities Council

Spatial Characterisation

Generally speaking there is an inverse relationship between resolving power and sensitivity.

Sensitivity

$$S = \frac{\int f(E)\exp(-\sigma\rho\ell)\,dE}{mm^2}\cdot\kappa\cdot\frac{NA^2}{4\eta^2}\cdot\frac{A_{px}(mm^2)}{M_o}$$

Photons produced in scintillator per area	Lens collection efficiency	Distributed over pixels

Resolving Power

$$R = \sqrt{\left(\frac{p}{NA}\right)^2 + (q\ell NA)^2 + \left(\frac{2dx}{NA}\right)^2 + \sigma_e^2}$$

Defect of focus, diffraction, spherical aberration	Nyquist limit, energy deposition

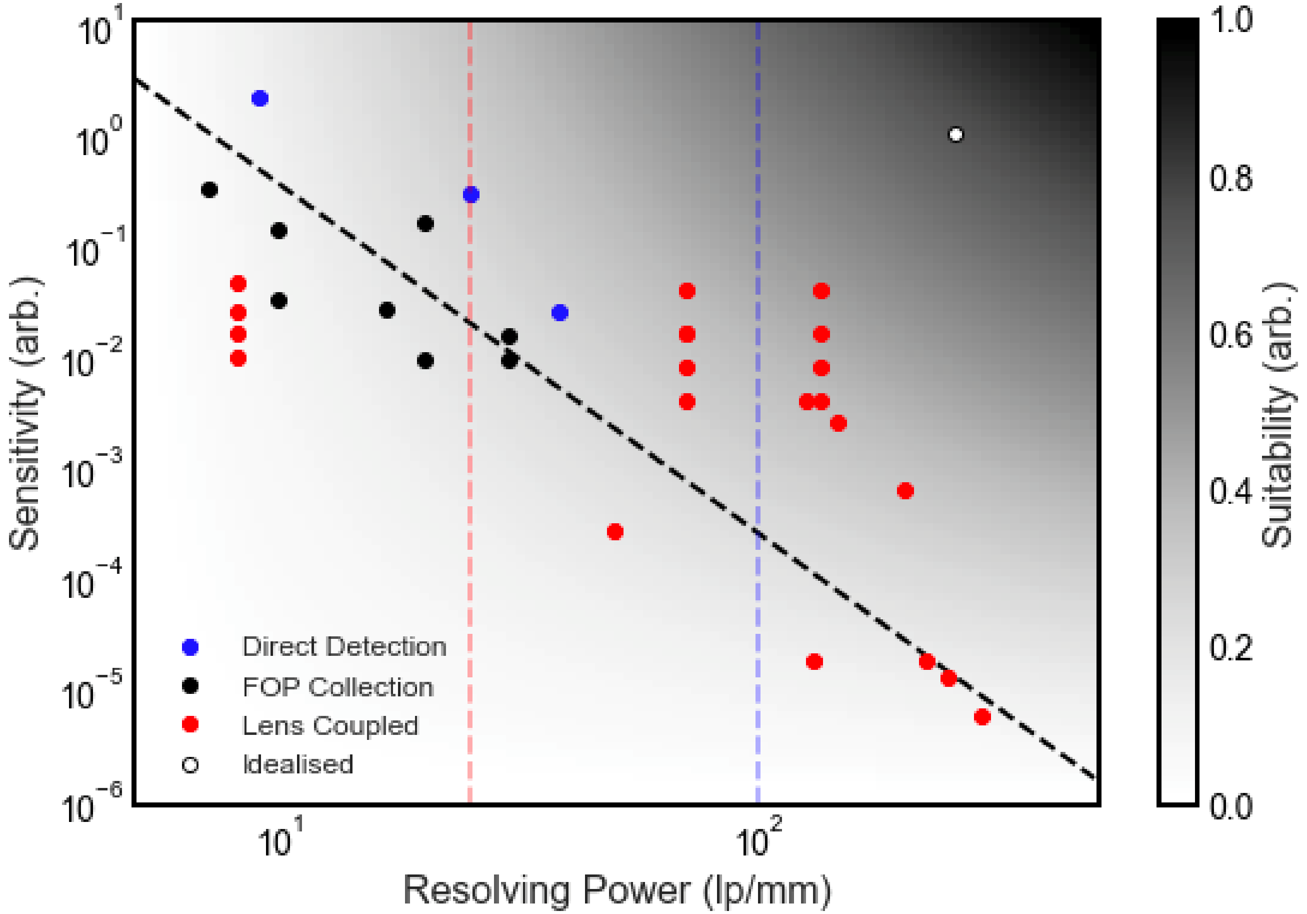

Penumbral Measurements

Attenuating (knife/rolled/wire) edge positioned in the beam blocks part of the source, the transition from light to dark is a measure of the source profile.

$$M = \frac{x'}{x} \rightarrow y = \frac{y'}{M}$$

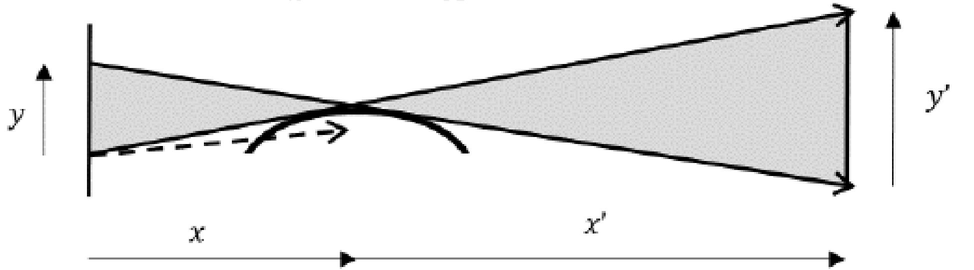

Kniep *et al.* Phys. Rev. ST Accel. Beams 15, 021302 (2012)

J. Wood, Diss. Imperial College London, (2017)

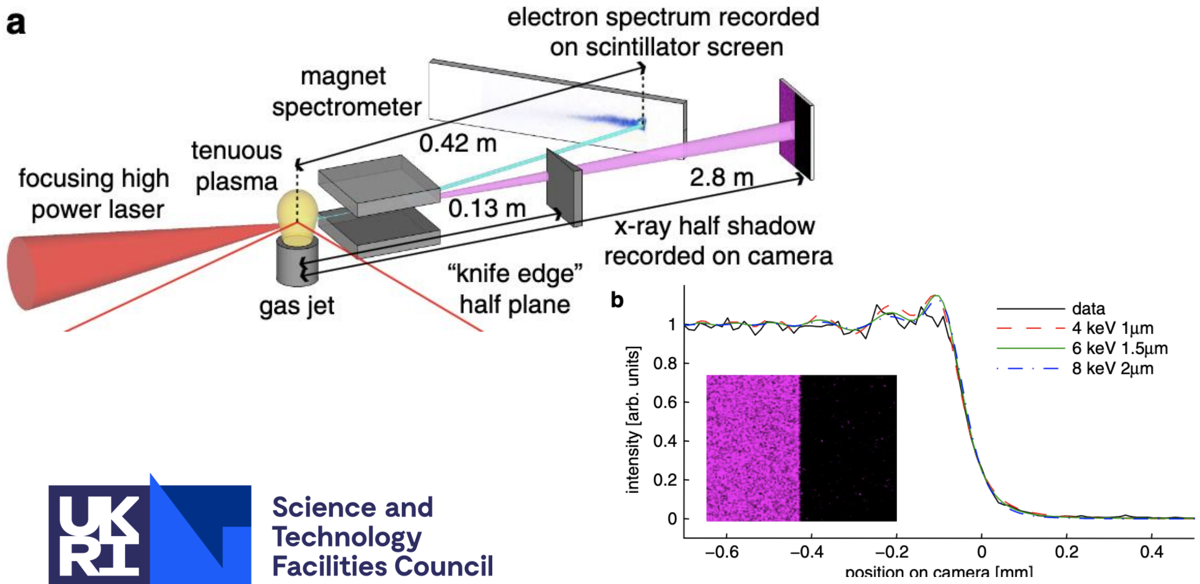

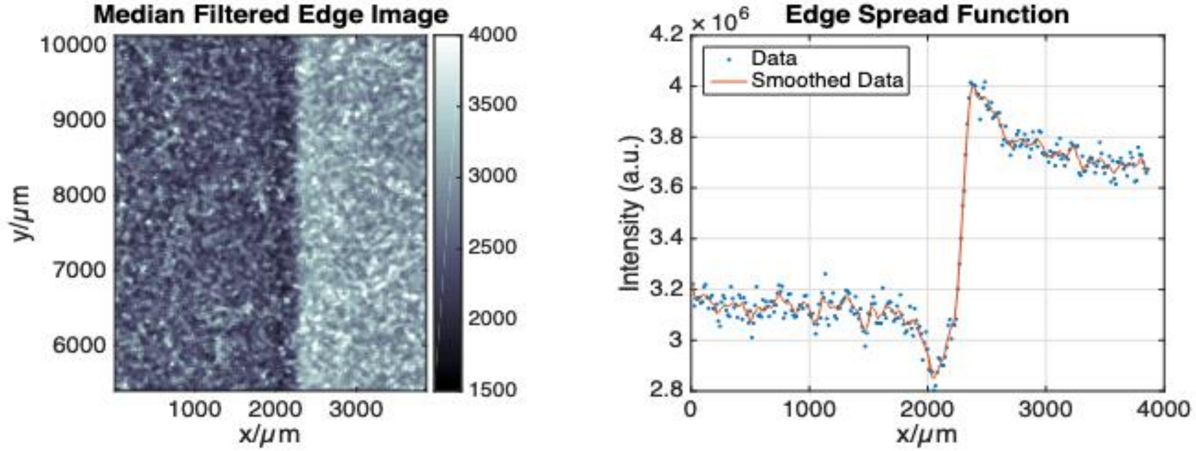

Penumbral Measurements

For laser solid bremsstrahlung, this approach demonstrated a complexity to sources.

There is not only a narrow source but a broader second distribution that can extend up to the width of the target foil. This is due to the recirculation of electrons in the target, those on the first pass all contribute to the central emission, a fraction of these recirculate and spread into the rest of the target driving a second less intense x-ray source.

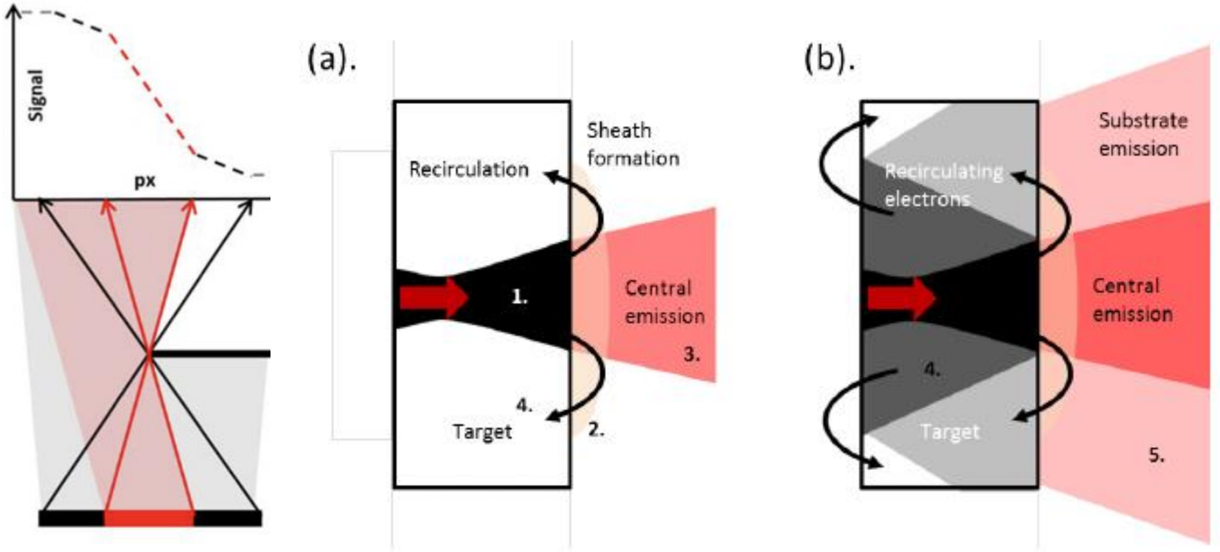

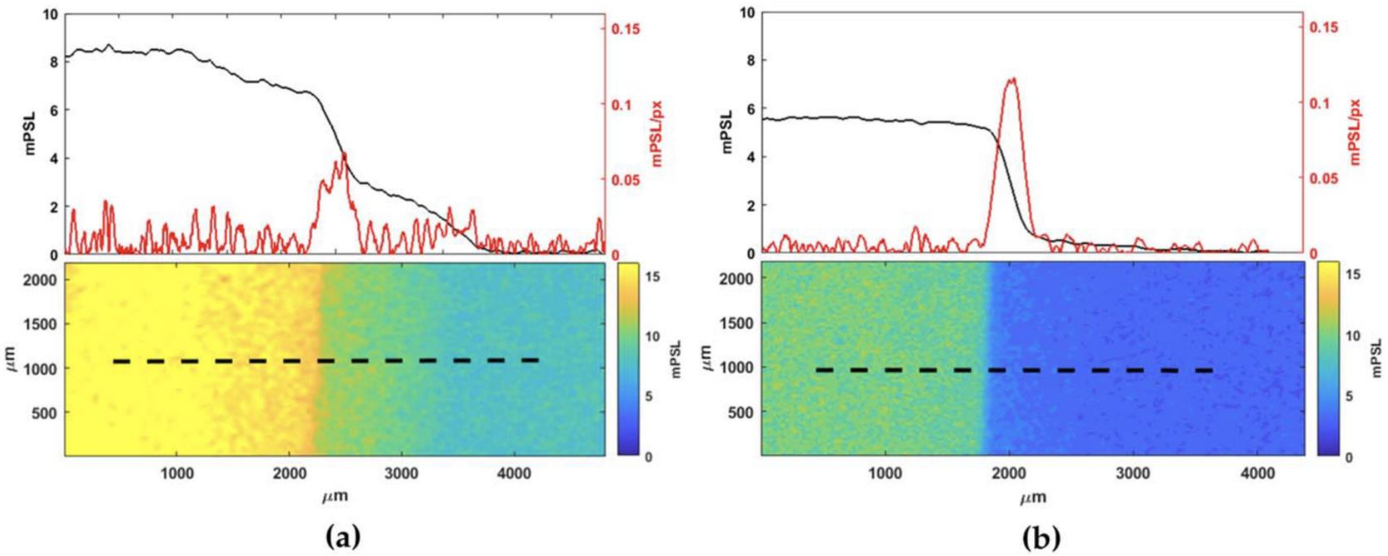

Science and Technology Facilities Council

Corde *et al.* PRL 107, 215004 (2011)

Penumbral Measurements

Expanding this to an aperture, or complex shape, (or coded aperture..) allows a more complete picture of the source to be built up.

Adrian et al. RSI. **92**, 043548 (2021)

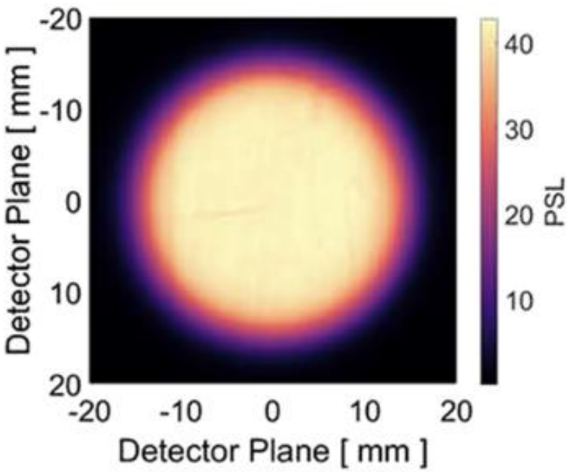

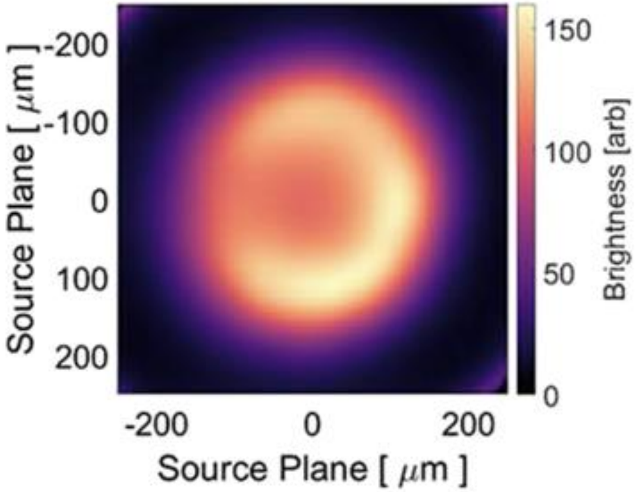

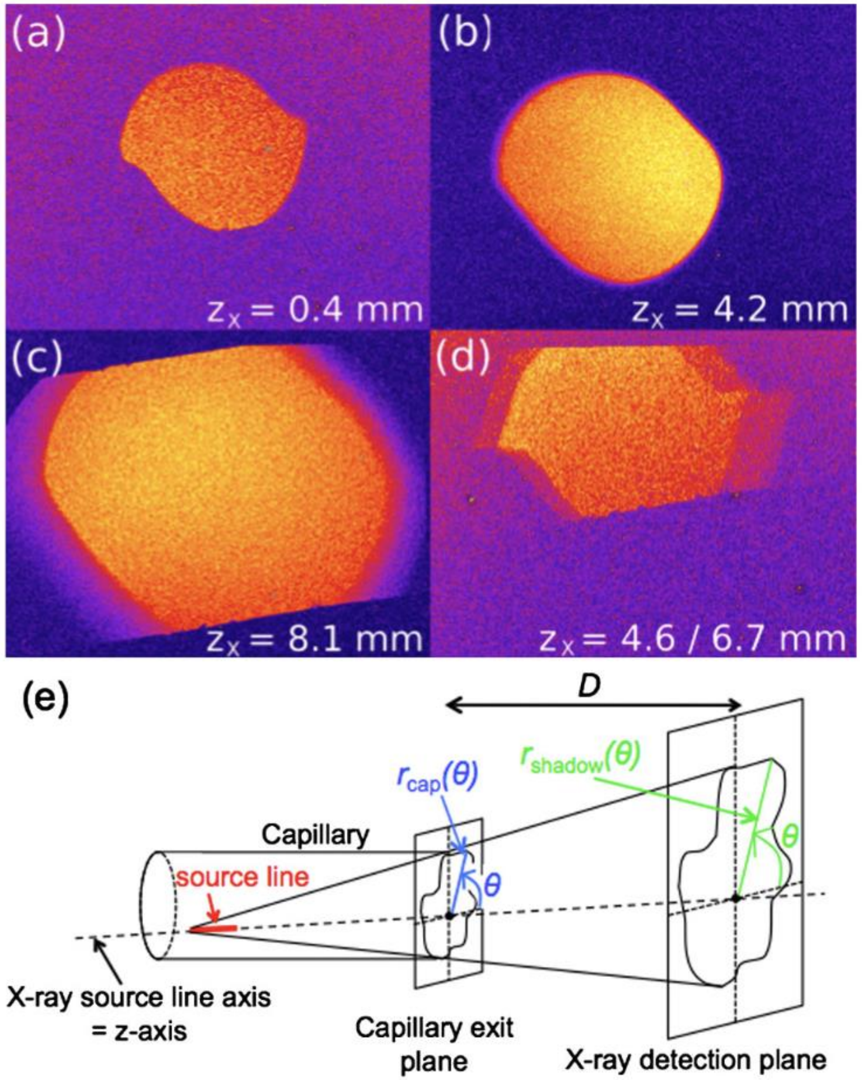

Inference by radiography

One clear way to demonstrate the emission area of x-ray sources is to perform a radiograph of a known/characterisation sample. We again fall into the trap of becoming detector limited however it sets an upper bound on the source area.

LWFA Betatron

$< 4\ \mu m$ near beam centre

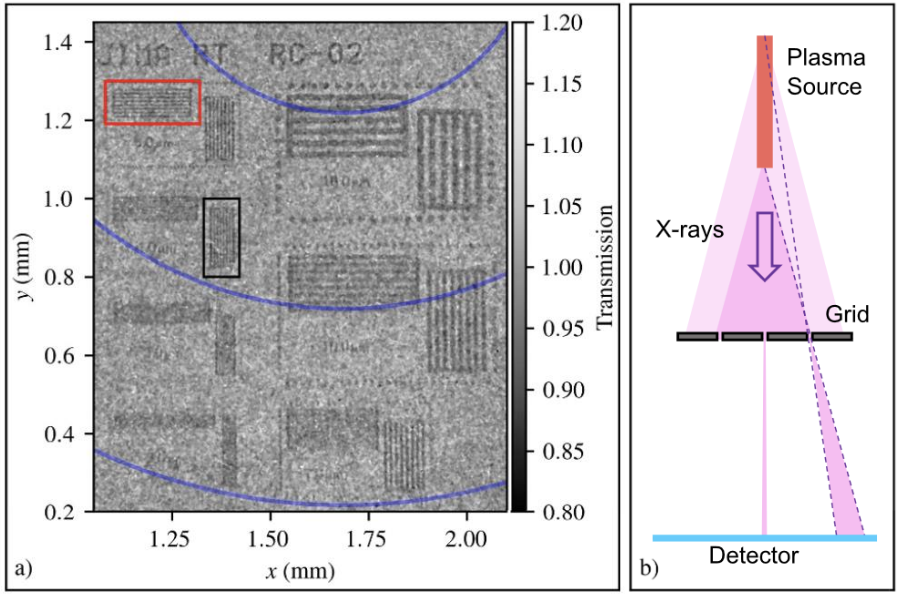

Finlay *et al* PPCF **63** (2021) 084010

LPI Bremsstrahlung

$< 200um$ for 100um thick Ta target

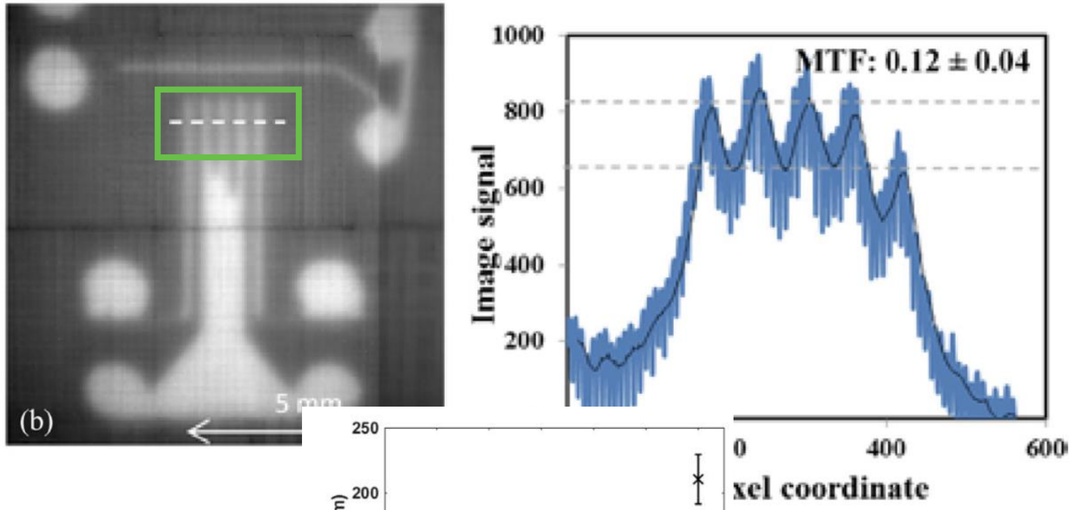

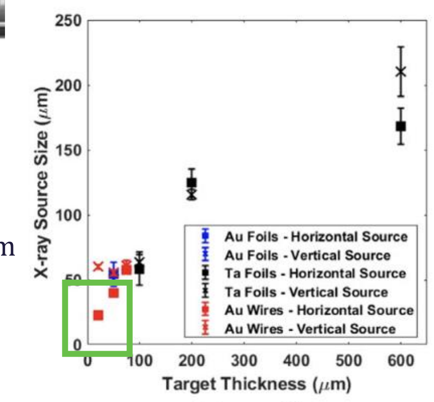

(a) Source Size

Measured at 20 µm for wire target

Brenner *et al.* PPCF **58** (2016) 014039

Inference by radiography

LWFA Bremsstrahlung

$< 150\ \mu m$ on single shot

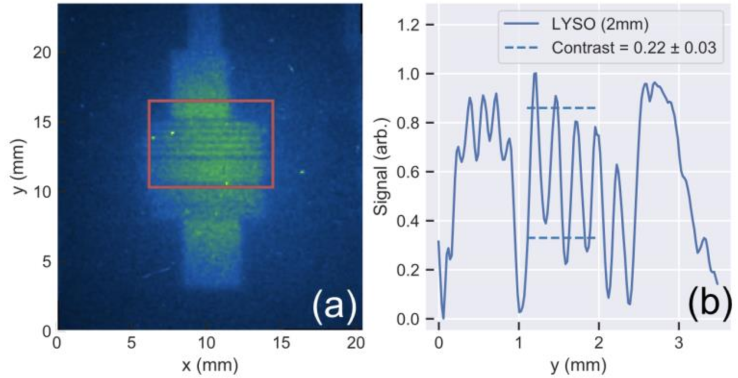

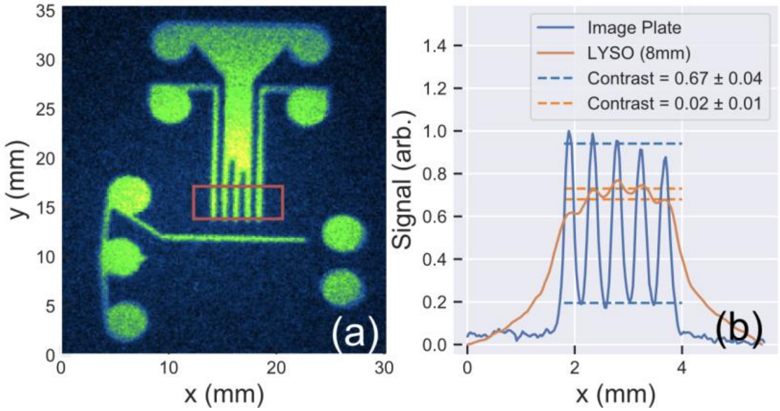

High contrast $\sim 200um$ from multi-shot accumulation

Underwood *et al.* PPCF **62** (2020) 124002

ICS

$< 20um$ for 80 integrated shots, $\sim 1\mu m$ for single shot

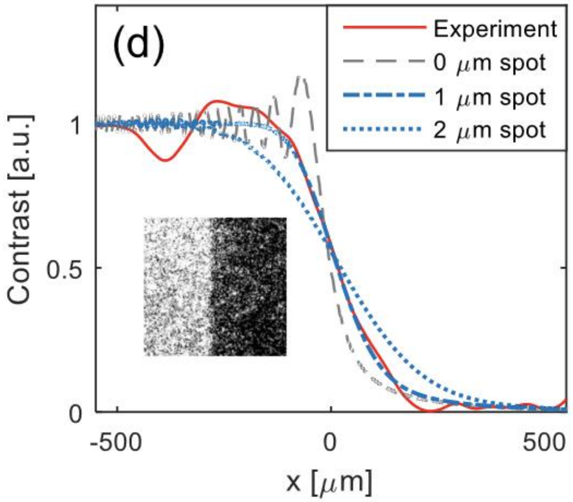

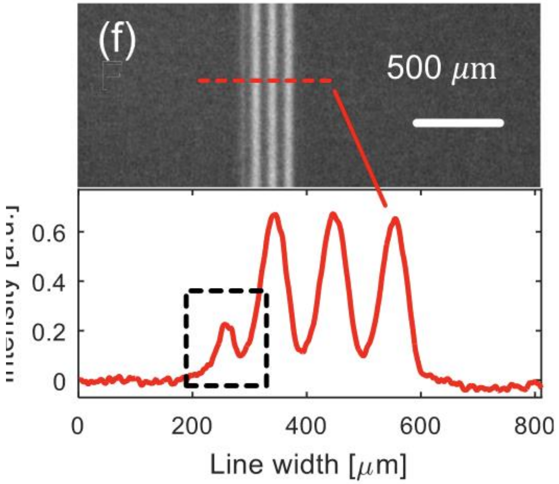

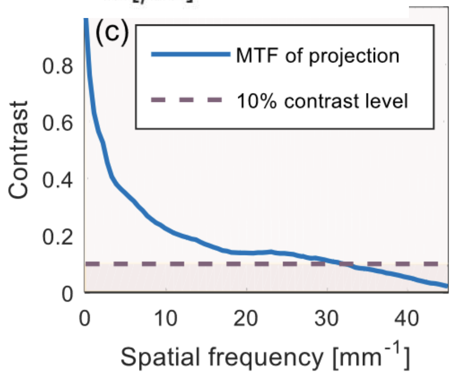

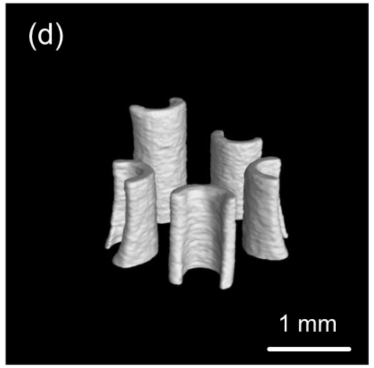

Y. Ma *et al.* Matter and Radiation at Extremes **5**, 064401 (2020)

Science and Technology Facilities Council

Science and Technology Facilities Council

Summary

Multiple mechanisms to generate x-rays with lasers.

Many techniques to characterise the emission both spectrally and spatially.
Although there are traps with each route that we must be aware of.

Regardless, **laser driven x-rays are a powerful and flexible source of radiation**

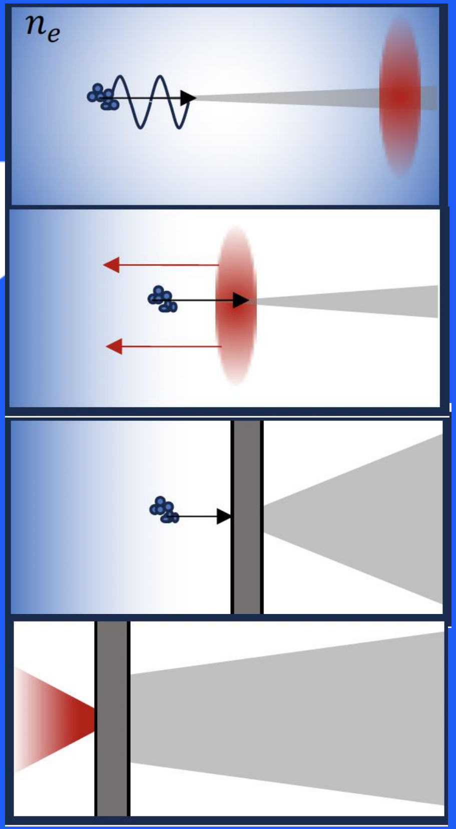

Betatron

ICS

LWFA Brems

LPI Brems

See the next talk by S. Cippiccia for a look into the applications of these sources!

Science and Technology Facilities Council

Thank you

Science and Technology Facilities Council

@STFC_matters

Science and Technology Facilities Council